Sensor and Simulation Notes

Note XXII
6 June 1966

A Transmission Line EMP Simulation Technique for Buried Structures

1/Lt Carl E. Baum

Air Force Weapons Laboratory

Abstract

A transmission line consisting of vertical conductors buried in the ground is evaluated from the viewpoint of reproducing part of the electromagnetic field distribution from a large distributed source at the ground surface (e.g., the nuclear EMP). When combined with the appropriate electromagnetic energy sources, this is a possible EMP simulation technique for use with buried structures.

I. Introduction

When considering the vulnerability of a large, complex, buried installation to the nuclear electromagnetic pulse (EMP), we need some technique for simulating this pulse; i.e., a means of artifically producing electromagnetic fields with a temporal and spatial variation (over the extent of the site) similar to that expected from the EMP.

Consider the geometry of figure 1 in which we have some buried structure to be tested. We assume the ground to be characterized (electrically) by a permeability, μ, a permittivity, ε, and a conductivity, σ.[1] In general the fields in this ground will then be propagating at a velocity significantly slower than c, the speed of light in vacuum. However, fields will appear over the air-ground interface at close to c either because outside the nuclear source region we have an electromagnetic wave propagating over the interface or because inside the nuclear source region where the air conductivity can be high (even comparable to the ground) the field sources move over the interface at some significant fraction of c. Thus, in the ground, the fields will propagate very nearly perpendicular to the ground surface, i.e, in the negative z direction.

There are certain limitations to this model. In some cases we may have to limit the horizontal extent (2a or 2b) of our consideration to distances smaller than those over which the field above the surface changes significantly (such as the gamma-ray mean free path of around 200 meters), or we may have to limit our frequencies of interest to those for which the skin depth in the ground is also smaller than such distances. Keeping these possible limitations in mind we shall take as our model for the field distribution in the ground one based on a wave propagating in the negative z direction.

Define the x axis as the direction of the magnetic field and the y axis as the direction of the electric field for this wave propagating into the ground. Let us then place conductors (plates or rods) perpendicular to the y axis (or parallel to the x, z plane). These conductors, being perpendicular to the electric field, do not disturb this wave assumed propagating in the negative z direction.

Consider a parallel plate structure, or more practically two parallel grids of conducting rods or stakes, each grid of width, 2a, separated by a distance, 2b, and of depth, ℓ, as illustrated in figure 1. If we drive this structure from the top as a transmission line, then near the axis of the transmission line (ignoring the presence of a buried structure being tested) we will have a fairly uniform field pattern for a given z, similar to the EMP.[2] However, there are other limitations to consider.

There are in general fringing fields, near the top and bottom of the transmission line, which limit our model in these regions unless we compensate for these distortions. For our calculations we assume that the length, ℓ, is much larger than either horizontal dimension, 2a or 2b. Associated with the horizontal dimensions we also have transit time limitations, i.e., it takes a certain time for a signal from the generator to distribute over the horizontal dimensions of the transmission

1. Rationalized m.k.s. units are used throughout.
2. For a discussion of this kind of field pattern see SSN XXI, Impedances and Field Distributions for Parallel Plate Transmission Line Simulators, by this author.

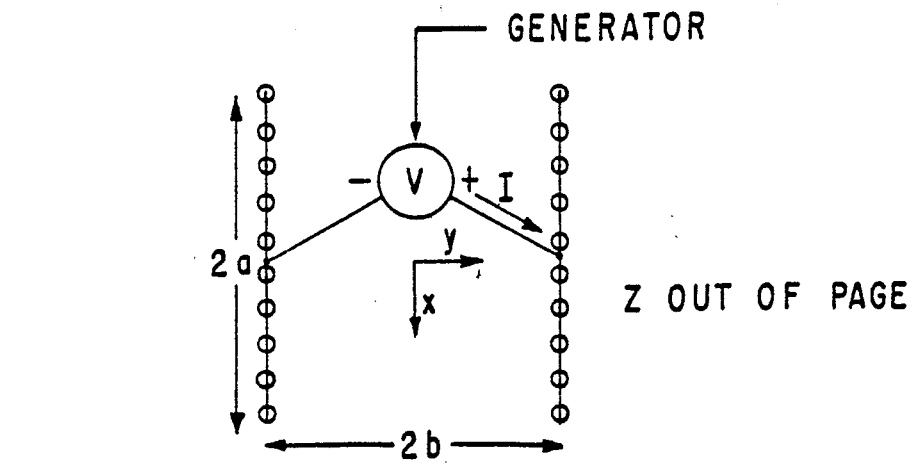

A. TOP VIEW

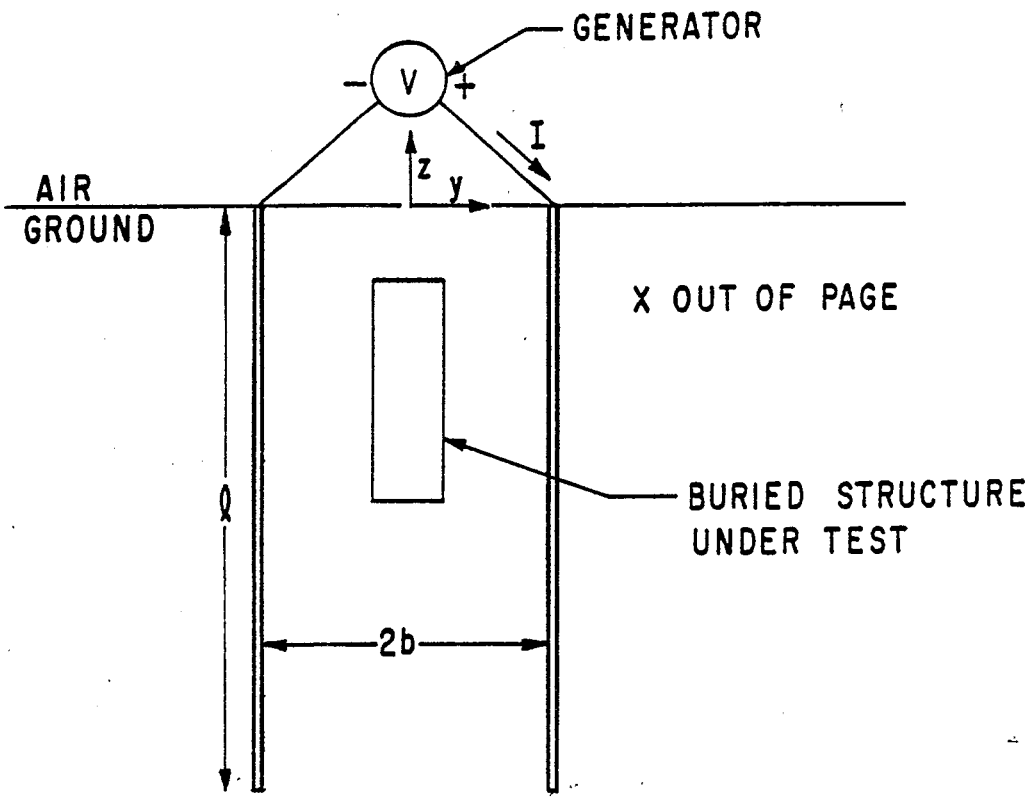

B. SIDE CROSS SECTION

FIGURE 1 TRANSMISSION LINE IN GROUND

line. Our calculations will apply only for signals with characteristic times much longer than such transit times over the ground surface. This problem of simulating these higher frequencies over the ground surface is planned to be considered in future notes. We must also insure that the conductors forming the transmission line make good electrical contact with the ground so that the TEM propagation mode in this lossy medium is not significantly distorted, altering our desired field distribution.

If the transmission line in the lossy ground were infinitely long, then a signal from the generator would propagate along the transmission line in a manner similar to the propagation of the EMP into the ground. However, the transmission line cannot practically be infinitely long. In general it would seem difficult to terminate a finite length of this transmission line in its characteristic impedance since for the case of $\sigma >> \omega\varepsilon$, and μ and σ independent of the radian frequency, ω, the characteristic impedance varies as $\sqrt{\omega}$. In addition, it may be difficult in some cases to have access to the bottom of the transmission line to connect any kind of terminator. In this case, it will probably be necessary to leave the bottom of the transmission line unterminated as indicated in figure 1.

Since we limit our concern to the case of $\sigma >> \omega\varepsilon$ in the ground then an unterminated (or open circuited) transmission line will not be that bad for reproducing a desired field distribution in the ground. There are no sharp reflection or resonance characteristics as in an open-circuited, non-lossy transmission line. For skin depths in the ground much smaller than the length of the transmission line, the reflection from the bottom attenuates rapidly on the way up, becoming insignificant and the finite-length, unterminated transmission line behaves as one of infinite length. For skin depths much larger than ℓ the transmission line impedance behaves as lumped circuit elements. Likewise, the fields assume a certain distribution with depth which differs from the field distribution for such depths on an infinite length transmission line. In this note we calculate the approximate variation of these fields with depth, frequency, and time.

Consider the variation of the impedance of the open-circuited transmission line with frequency (or skin depth) in a very lossy ($\sigma >> \omega\varepsilon$) soil as well as the variation of the fields with depth, frequency, and time. We also consider the variation of the same quantities on a short-circuited transmission line, which represents one of the simpler terminations (shorting conductors across the bottom of the transmission line) which we might consider attempting. In each of these cases we compare the results to those obtained on the infinite length transmission line which represents the "ideal" case we are trying to approximate. With such a comparison we can see for a given observation depth, -z, (relative to the length, ℓ) how significantly the magnetic field and electric field (or current density) are distorted relative to their "ideal" values. For convenience the permeability and conductivity of the ground are assumed independent of both frequency and location and both impedances and fields are presented in normalized form, the fields being normalized to a unity magnetic field at the surface, $z = 0$. Based on these calculations we can choose the depth of the transmission line for an EMP simulation test on a given buried structure.

There is another important limitation of this technique in that the structure under test may be quite extensive, particularly if we consider electrical connections (cable runs) to and from the structure which may of necessity extend beyond the area covered by the buried transmission line. In such cases, the structure itself may strongly influence the field distribution in the ground. To some extent we may be able to partially compensate for this perturbation by altering the cross section of the transmission line to more closely match the field pattern (around the structure) we might expect from the EMP. However, in the case of some complex sites it may be very difficult to estimate the effect of such perturbations and we may have to rely on measurements of the field distribution at various positions in the transmission line during the test to determine how closely we have approximated the field distribution expected from the EMP.

We do not consider the actual time variation of the fields which might be produced by various electrical energy sources when attached to this type of transmission-line simulator. We hope to discuss such problems in future notes.

II. Impedance of the Buried Transmission-Line Simulator

Considering first the impedance of this transmission line in the ground, we have a wave impedance

$$Z = \left|\frac{s\mu}{\sigma+s\varepsilon}\right|^{1/2} \tag{1}$$

where the Laplace transform variable, s, can be replaced by $j\omega$ for a frequency analysis. This can be related to the impedance of an infinitely long transmission line, Z_{L_∞}, by a geometric factor, f_g, as

$$Z_{L_\infty} = f_g Z \tag{2}$$

We also have electromagnetic waves on the transmission line (for single frequencies) of the form $e^{j\omega t \mp jkz}$ where the propagation constant, k, is

$$k = [-s\mu(\sigma+s\varepsilon)]^{1/2} \tag{3}$$

We have presumed that the electrical parameters of the ground do not vary over the extent of the transmission line.

For the case of $\sigma >> \omega\varepsilon$ for all frequencies of interest (for this note) we have the simpler expressions

$$Z \approx \left|\frac{s\mu}{\sigma}\right|^{1/2} \tag{4}$$

and

$$k \approx (-s\mu\sigma)^{1/2} \tag{5}$$

In the frequency domain we can use some parameters, such as the skin depth, δ, which is

$$\delta = \sqrt{\frac{2}{\omega\mu\sigma}} \tag{6}$$

and thus

$$Z \simeq \left(j\frac{\omega\mu}{\sigma}\right)^{1/2} = \frac{1+j}{\delta\sigma} \tag{7}$$

and

$$k \simeq (-j\omega\mu\sigma)^{1/2} = \frac{1-j}{\delta} \tag{8}$$

Carrying this one step further define a normalized skin depth, δ', as

$$\delta' = \frac{\delta}{\ell} \tag{9}$$

where ℓ is the depth of the transmission line.

The impedance of the infinite or ideal transmission line is now

$$Z_{L_\infty} \simeq f_g \frac{1+j}{\delta\sigma} \tag{10}$$

or in normalized form for comparison with the other cases

$$\frac{\ell\sigma}{f_g} Z_{L_\infty} \simeq \frac{1+j}{\delta'} \tag{11}$$

On the open-circuited transmission line we have a positive voltage reflection and a negative current reflection at the bottom of the transmission line giving an impedance, Z_{L_o}, as

$$Z_{L_o} = Z_{L_\infty} \frac{1+e^{-j2k\ell}}{1-e^{-j2k\ell}} \tag{12}$$

or in normalized form

$$\frac{\ell\sigma}{f_g} Z_{L_o} \simeq \frac{1+j}{\delta'} \frac{1+e^{-2\frac{1+j}{\delta'}}}{1-e^{-2\frac{1+j}{\delta'}}} \tag{13}$$

On the short-circuited transmission line we have a negative voltage reflection and a positive current reflection at the bottom of the transmission line giving an impedance, Z_{L_s}, as

$$Z_{L_s} = Z_{L_\infty} \frac{1-e^{-j2k\ell}}{1+e^{-j2k\ell}} \tag{14}$$

or in normalized form

$$\frac{\ell\sigma}{f_g} Z_{L_s} \simeq \frac{1+j}{\delta'} \frac{1-e^{-2\frac{1+j}{\delta'}}}{1+e^{-2\frac{1+j}{\delta'}}} \tag{15}$$

These normalized impedances (equations (11), (13), and (15)) are plotted against δ' in figures 2 through 5, considering their magnitudes, phases, real parts, and imaginary parts in that order. From these graphs we can see that for frequencies such that the skin depth is less than the depth of the transmission the impedances all look about the same, i.e., the finite length has little influence and the impedances behave as if the transmission line were infinitely long. However, for frequencies such that the skin depth is greater than the depth of the transmission line., the results are quite different from one another. Thus, let us consider the asymptotic forms of the impedances of these finite-length transmission lines for large δ'.

For the open-circuited transmission line we have from equation (13)

$$\frac{\ell\sigma}{f_g} Z_{L_o} \approx \frac{1+j}{\delta'} \coth\left(\frac{1+j}{\delta'}\right) \tag{16}$$

Expanding this for large δ', we have

$$\frac{\ell\sigma}{f_g} Z_{L_o} \approx \frac{1+j}{\delta'}\left[\frac{\delta'}{1+j} + \frac{1+j}{3\delta'}\ldots\right]$$

$$\approx 1 + j\,\frac{2}{3}\,\delta'^{-2} \tag{17}$$

For large δ' we can then write this impedance as

$$Z_{L_o} \approx f_g\left[\frac{1}{\ell\sigma} + j\,\frac{\omega\mu\ell}{3}\right] \tag{18}$$

or let

$$Z_{L_o} \approx R_o + j\omega L_o \tag{19}$$

where

$$R_o = f_g \frac{1}{\ell\sigma} \tag{20}$$

and

$$L_o \approx f_g \frac{\mu\ell}{3} \tag{21}$$

Thus, for low frequencies ($\delta'>>1$) we can represent the impedance of the transmission line, with an open-circuited termination, as the series combination of a resistance and an inductance.

For the short-circuited transmission line we have from equation (15)

$$\frac{\ell\sigma}{f_g} Z_{L_s} \approx \frac{1+j}{\delta'} \tanh\left(\frac{1+j}{\delta'}\right) \tag{22}$$

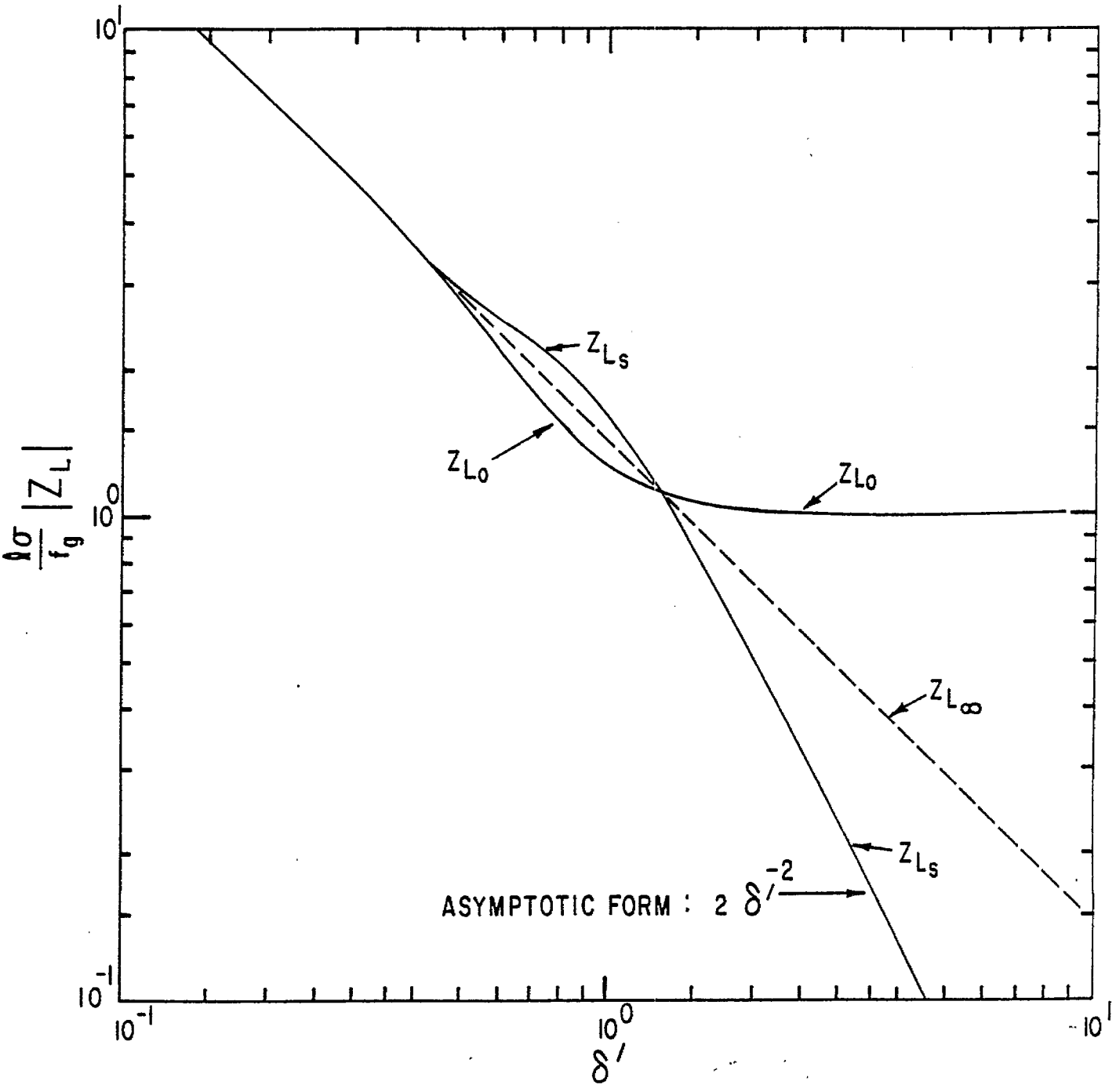

FIGURE 2. NORMALIZED MAGNITUDE OF TRANSMISSION LINE IMPEDANCE

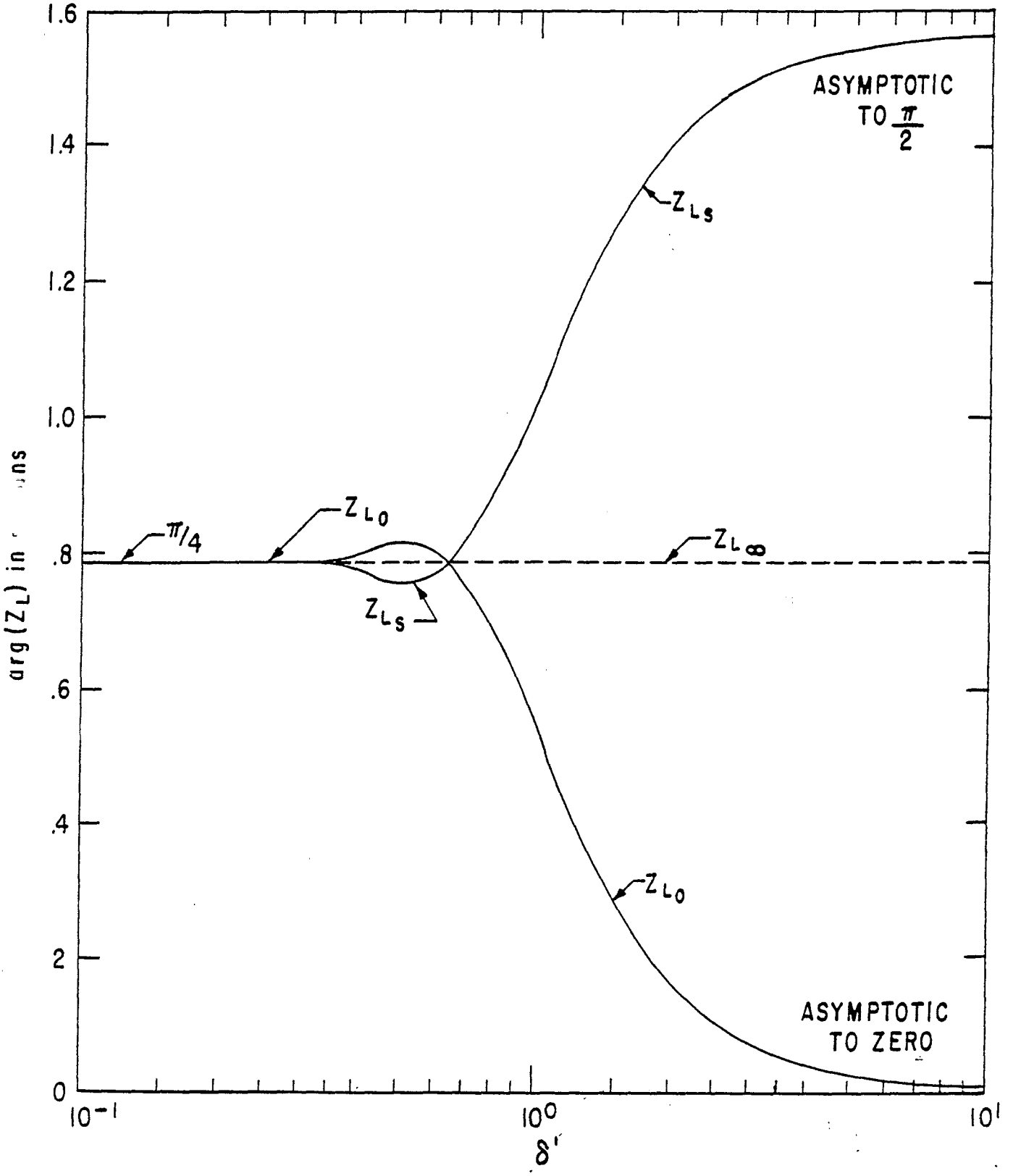

FIGURE 3. PHASE OF TRANSMISSION LINE IMPEDANCE

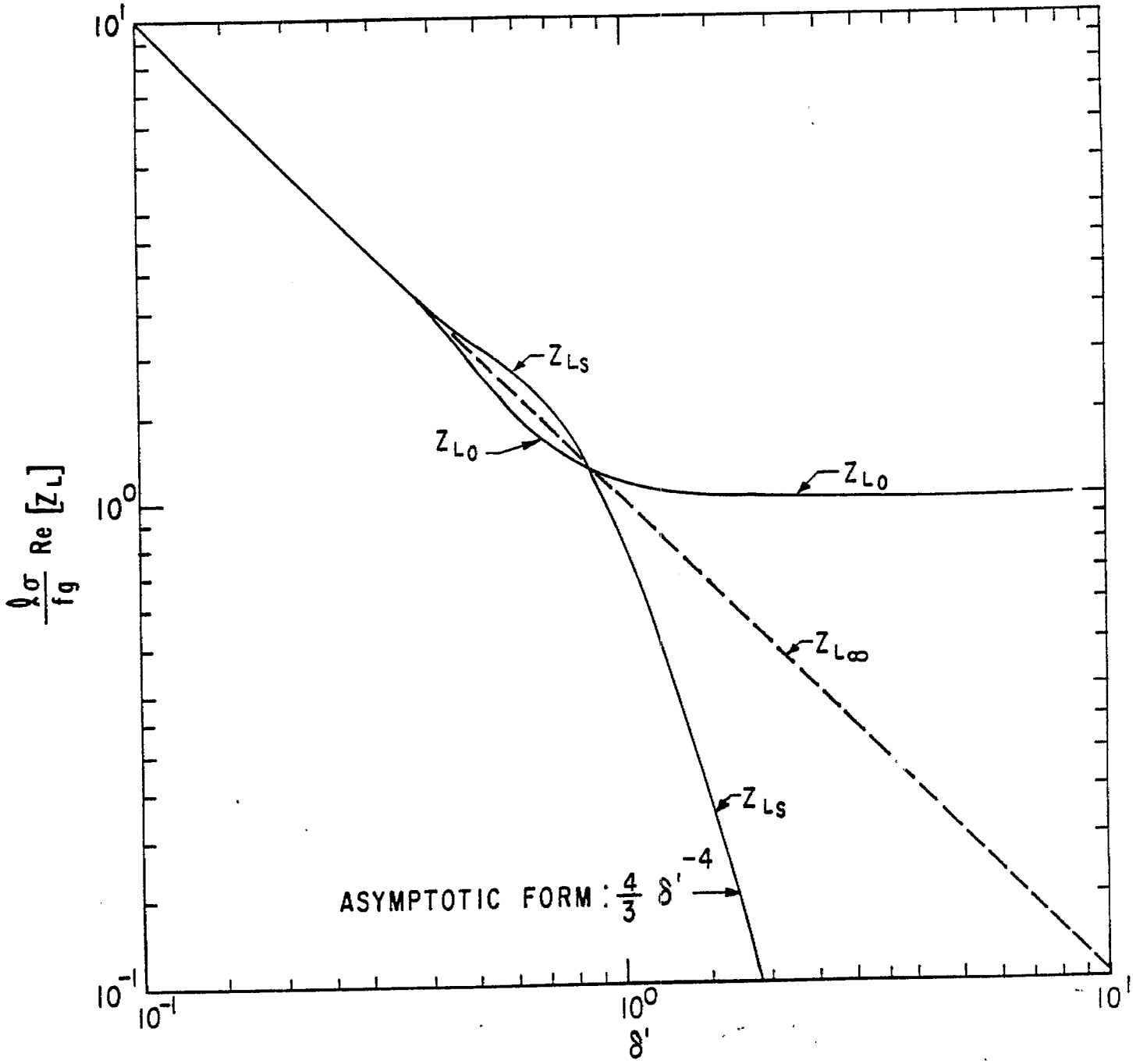

FIGURE 4. NORMALIZED REAL PART OF TRANSMISSION LINE IMPEDANCE

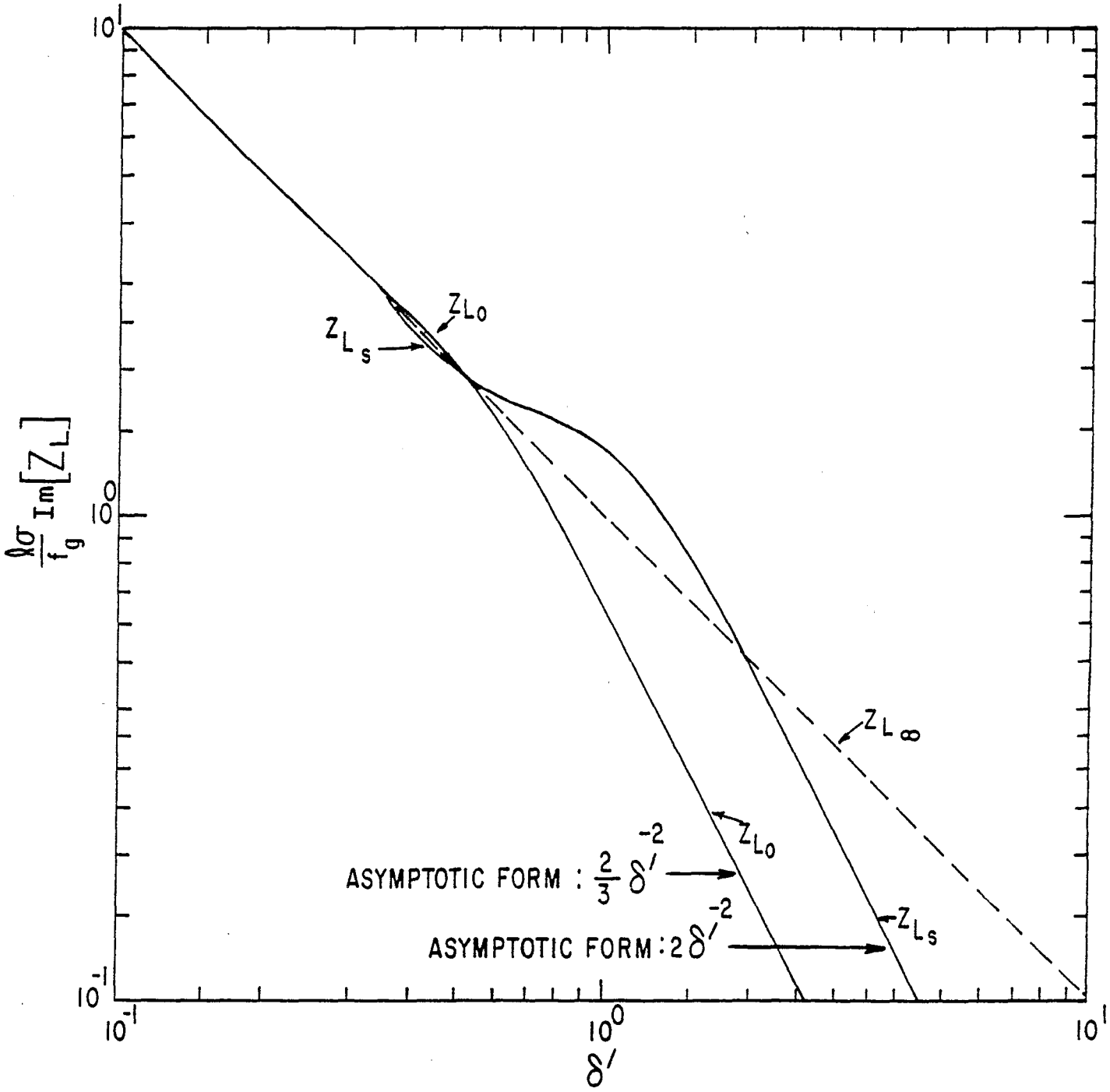

FIGURE 5. NORMALIZED IMAGINARY PART OF TRANSMISSION LINE IMPEDANCE

Expanding for large δ', we have

$$\frac{\ell\sigma}{f_g} Z_{L_s} \approx \frac{1+j}{\delta'} \left[\frac{1+j}{\delta'} - \frac{(1+j)^3}{3\delta'^3} \cdots \right]$$

$$\approx j2\delta'^{-2} + \frac{4}{3}\delta'^{-4} \tag{23}$$

Alternatively we can expand equation (22) as

$$\frac{\ell\sigma}{f_g} Z_{L_s} \approx \frac{1+j}{\delta'} \left[\frac{\delta'}{1+j} + \frac{1+j}{3\delta'} \cdots \right]^{-1}$$

$$\approx \left[-j \frac{\delta'^2}{2} + \frac{1}{3} \right]^{-1} \tag{24}$$

For large δ' we can then write this impedance as

$$Z_{L_s} \approx \left[\frac{1}{j\omega f_g \mu \ell} + \frac{\ell\sigma}{3 f_g} \right]^{-1} \tag{25}$$

or let

$$Z_{L_s} \approx \left[\frac{1}{j\omega L_s} + \frac{1}{R_s} \right]^{-1} \tag{26}$$

where

$$L_s = f_g \mu \ell \tag{27}$$

and

$$R_s = f_g \frac{3}{\ell\sigma} \tag{28}$$

Thus for low frequencies ($\delta' >> 1$) we can represent the impedance of the short-circuited transmission line as the parallel combination of an inductance and a resistance.

For the higher frequencies ($\delta' << 1$) then the finite length of the transmission line has little effect. However, for the lower frequencies ($\delta' >> 1$) the manner of terminating the finite-length transmission line has a significant effect, allowing us to characterize the impedance (for simple terminations) as a combination of lumped elements. These results will be important for combining the transmission line with electromagnetic energy sources and calculating field levels, waveforms, etc.

III. Fields in the Frequency Domain.

Now consider the field distributions on the transmission line in the frequency domain. For convenience we normalize all field distributions to the magnetic field at the top of the transmission line ($z = 0$). We also compare the field distributions for the finite-length transmission lines to those for the infinite-length transmission lines so that we can see over what range of positions and

frequencies the fields reproduce the "ideal" case. The calculations assume that the pertinent electrical parameters of the ground do not vary significantly over the extent of the transmission line and also that $\sigma >> \omega\varepsilon$ for all frequencies of interest.

Using the normalized parameters defined in the previous section, define also a normalized depth, z', as

$$z' = -\frac{z}{\ell} \tag{29}$$

where z' now varies between zero and one for the finite-length transmission line. The normalized magnetic field, h(z'), is related to the magnetic field, H(z'), by

$$h(z') = \frac{H(z')}{H(0)} \tag{30}$$

Similarly, we normalize (to the magnetic field) the electric field, e(z'), or better a normalized current density, j(z'), which are related by

$$j(z') = \sigma e(z') \tag{31}$$

and (in dimensionless form)

$$\ell j(0) = \left(\frac{\ell\sigma}{f_g} Z_L\right) h(0) \tag{32}$$

As with the impedance, Z_L, these three quantities are subscripted to indicate which of the transmission-line configurations is being considered.

For the infinite-length transmission line we have no reflections and thus just a wave of the form $e^{j\omega t + jkz}$. Suppressing $e^{j\omega t}$ in all solutions we then have for the normalized magnetic field

$$h_\infty(z') = e^{jkz} \approx e^{-(1+j)\frac{z'}{\delta'}} \tag{33}$$

and for the normalized current density

$$\ell j_\infty(z') = \left(\frac{\ell\sigma}{f_g} Z_{L_\infty}\right) h_\infty(z') \approx \frac{1+j}{\delta'} e^{-(1+j)\frac{z'}{\delta'}} \tag{34}$$

On the open-circuited transmission line the magnetic field (and current on the conductors) has a negative one reflection at the bottom giving a normalized magnetic field

$$h_o(z') = \frac{e^{jkz} - e^{-jk(2\ell+z)}}{1 - e^{-jk2\ell}} \approx e^{-(1+j)\frac{z'}{\delta'}} \frac{1 - e^{-2\frac{1+j}{\delta'}(1-z')}}{1 - e^{-2\frac{1+j}{\delta'}}} \tag{35}$$

This is graphed and compared with the normalized magnetic field on the infinite-length transmission line in figures 6 through 9. In figure 6 we have the magnitudes of h_o and h_∞ plotted vs. z' for specific δ' showing the distribution of magnetic field with depth. Figure 7 shows the relative phase of h_o and h_∞. In figures 8 and 9 we plot the magnitudes and relative phase against δ' for specific z'. For small δ' then h_∞ and h_o are about the same for all z' except near $z'=1$. However, for large δ' the two field distributions are comparable only near the top of the transmission line. Whereas, for large δ', h_∞ tends to a uniform distribution with depth, h_o tends to a linear decrease with depth becoming zero at the bottom. Based on these calculations we can decide the relative depths of the open-circuited transmission line and an observation point (or depth of an object to undergo EMP simulation) for a desired approximation of the magnetic field characteristics relative to those of the "ideal" case.

The current density (or electric field) on the open-circuited transmission line has a plus one reflection at the bottom giving (from equations (13) and (32))

$$\ell j_o(z') = \frac{e^{jkz} + e^{-jk(2\ell+z)}}{1 + e^{-jk2\ell}} \left(\frac{\ell\sigma}{f_g} Z_{L_o} \right) \qquad (36)$$

or

$$\ell j_o(z') = \frac{1+j}{\delta'} e^{-(1+j)\frac{z'}{\delta'}} \frac{1 + e^{-2\frac{1+j}{\delta'}(1-z')}}{1 - e^{-2\frac{1+j}{\delta'}}} \qquad (37)$$

This is graphed and compared with the normalized current density on the infinite transmission line (equation (34)) in figures 10 through 13. As with the magnetic field, j_o and j_∞ are nearly the same for small δ'. However, for large δ', j_o tends to one while j_∞ tends to zero for all z'. Thus, for large δ' the current density and electric field do not have the same ratio to the magnetic field as on the infinite-length transmission line. If this field ratio is important for an EMP simulation test then we may have to either use a more sophisticated termination for the transmission line or make ℓ large enough so that δ' is always less than one.

On the short-circuited transmission line the magnetic field (and the current on the conductors) has a plus one reflection at the bottom giving a normalized magnetic field

$$h_s(z') = \frac{e^{jkz} + e^{-jk(2\ell+z)}}{1 + e^{-jk2\ell}} = e^{-(1+j)\frac{z'}{\delta'}} \frac{1+e^{-2\frac{1+j}{\delta'}(1-z')}}{1+e^{-2\frac{1+j}{\delta'}}} \qquad (38)$$

Figures 14 through 17 compare this with h_∞. As with h_o, for small δ', h_s and h_∞ are about the same for all z' except near $z'=1$. For large δ' both h_s and h_∞ tend to one. However, for intermediate δ' (around

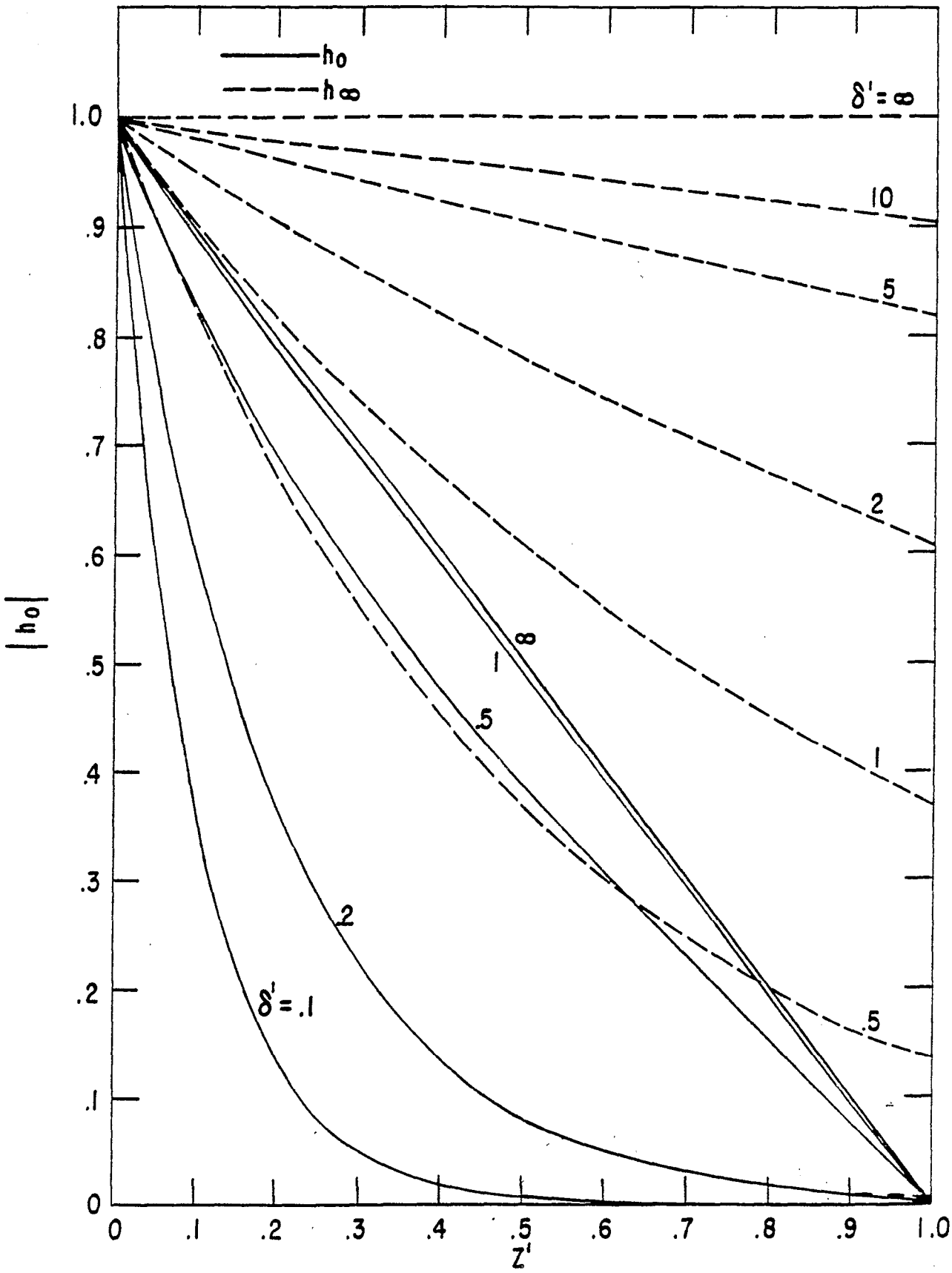

FIGURE 6 NORMALIZED MAGNITUDE OF MAGNETIC FIELD VS. DEPTH FOR OPEN-CIRCUITED TRANSMISSION LINE

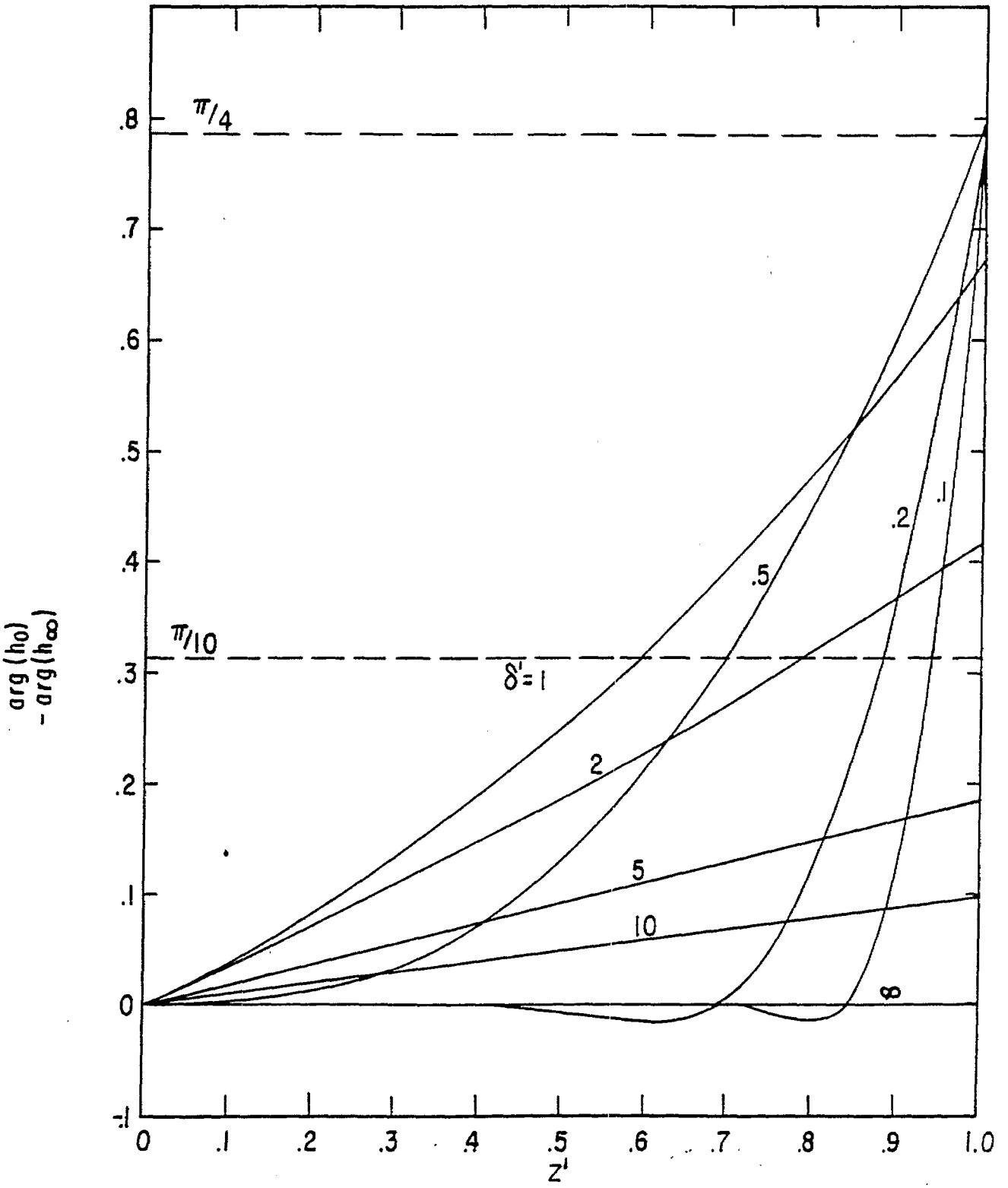

FIGURE 7 PHASE CHANGE OF MAGNETIC FIELD VS. DEPTH FOR OPEN-CIRCUITED TRANSMISSION LINE

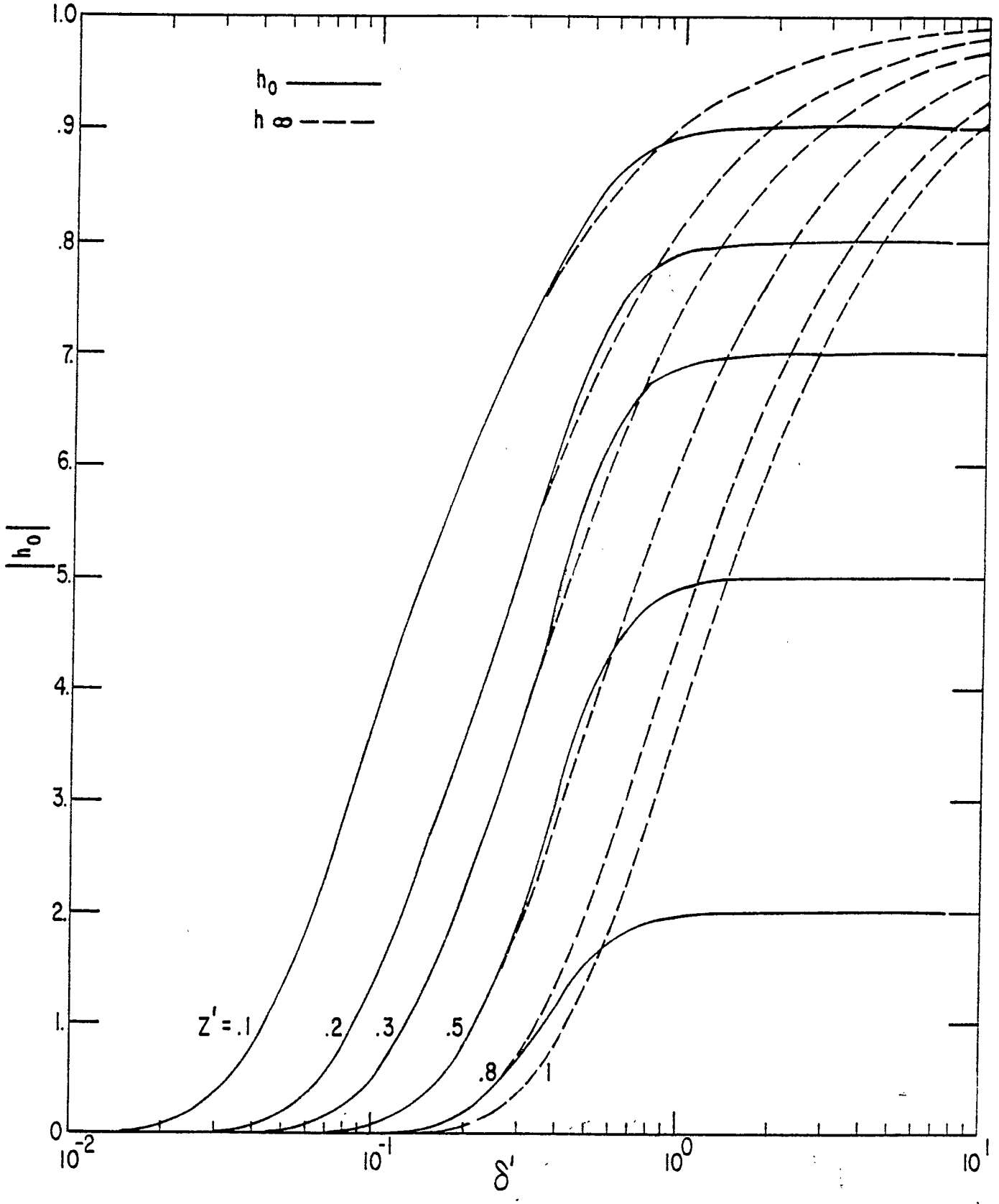

FIGURE 8. NORMALIZED MAGNITUDE OF MAGNETIC FIELD VS. SKIN DEPTH FOR OPEN-CIRCUITED TRANSMISSION LINE

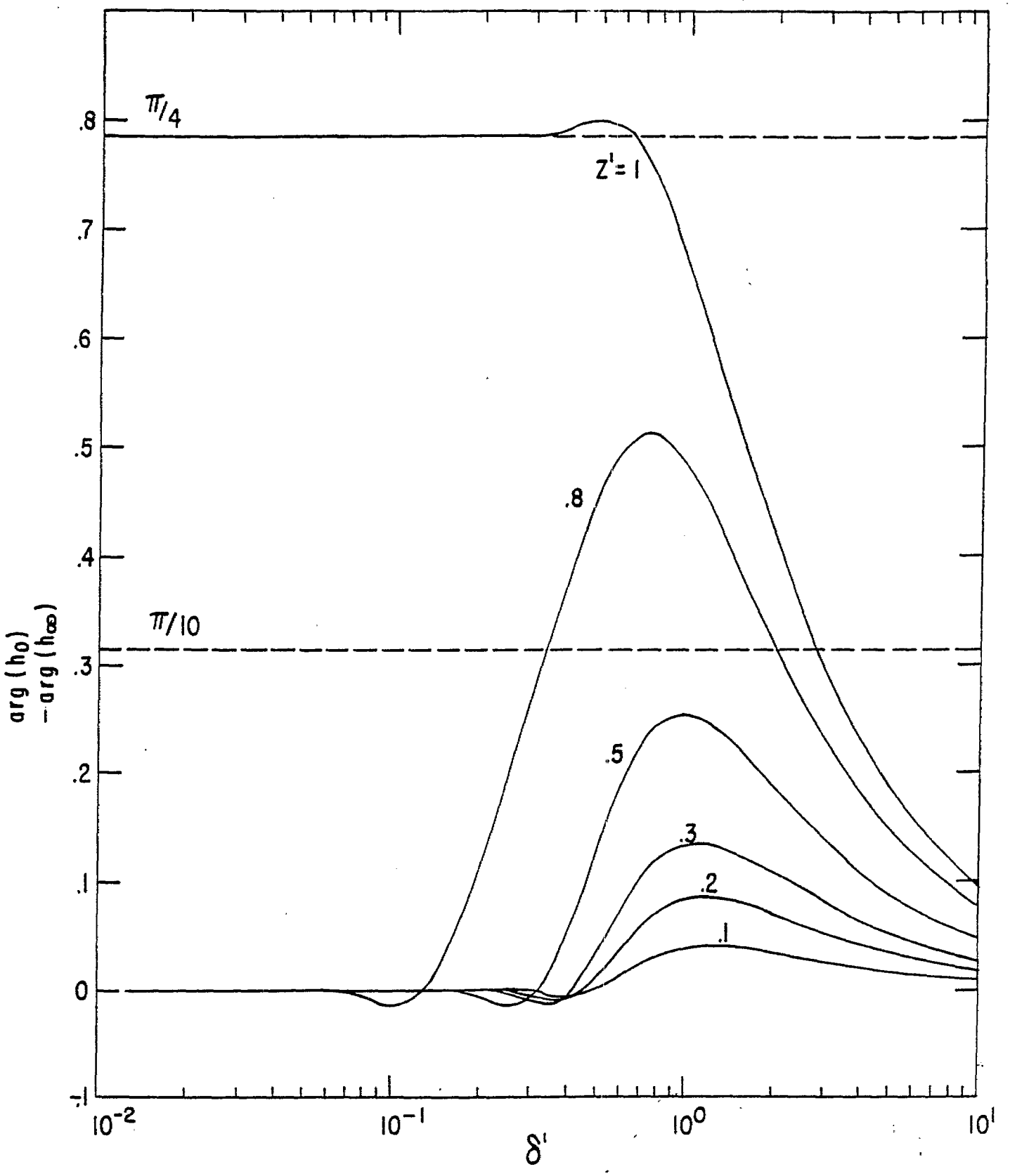

FIGURE 9 PHASE CHANGE OF MAGNETIC FIELD VS SKIN DEPTH FOR OPEN-CIRCUITED TRANSMISSION LINE

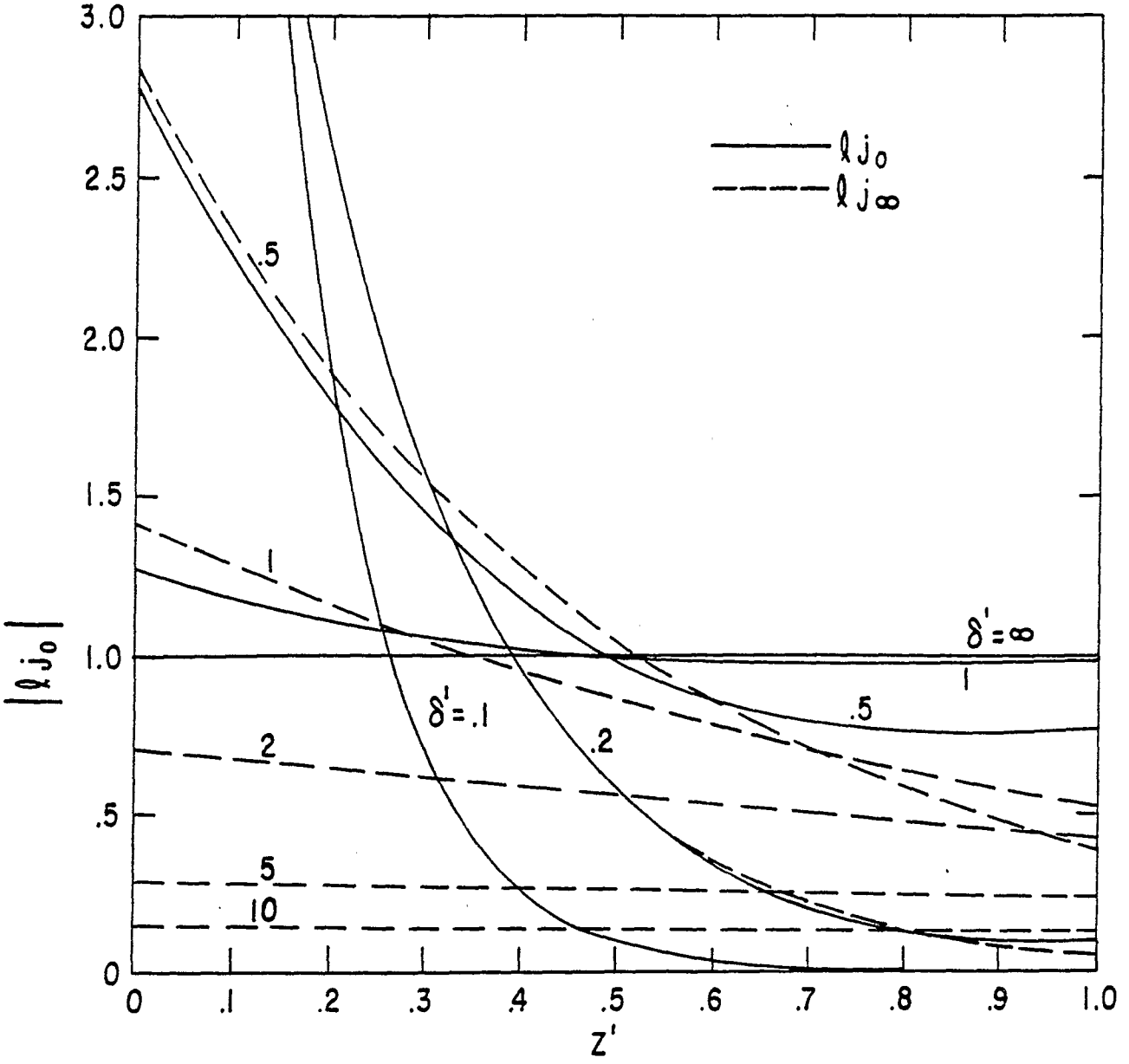

FIGURE 10 NORMALIZED MAGNITUDE OF CURRENT DENSITY VS. DEPTH FOR OPEN-CIRCUITED TRANSMISSION LINE

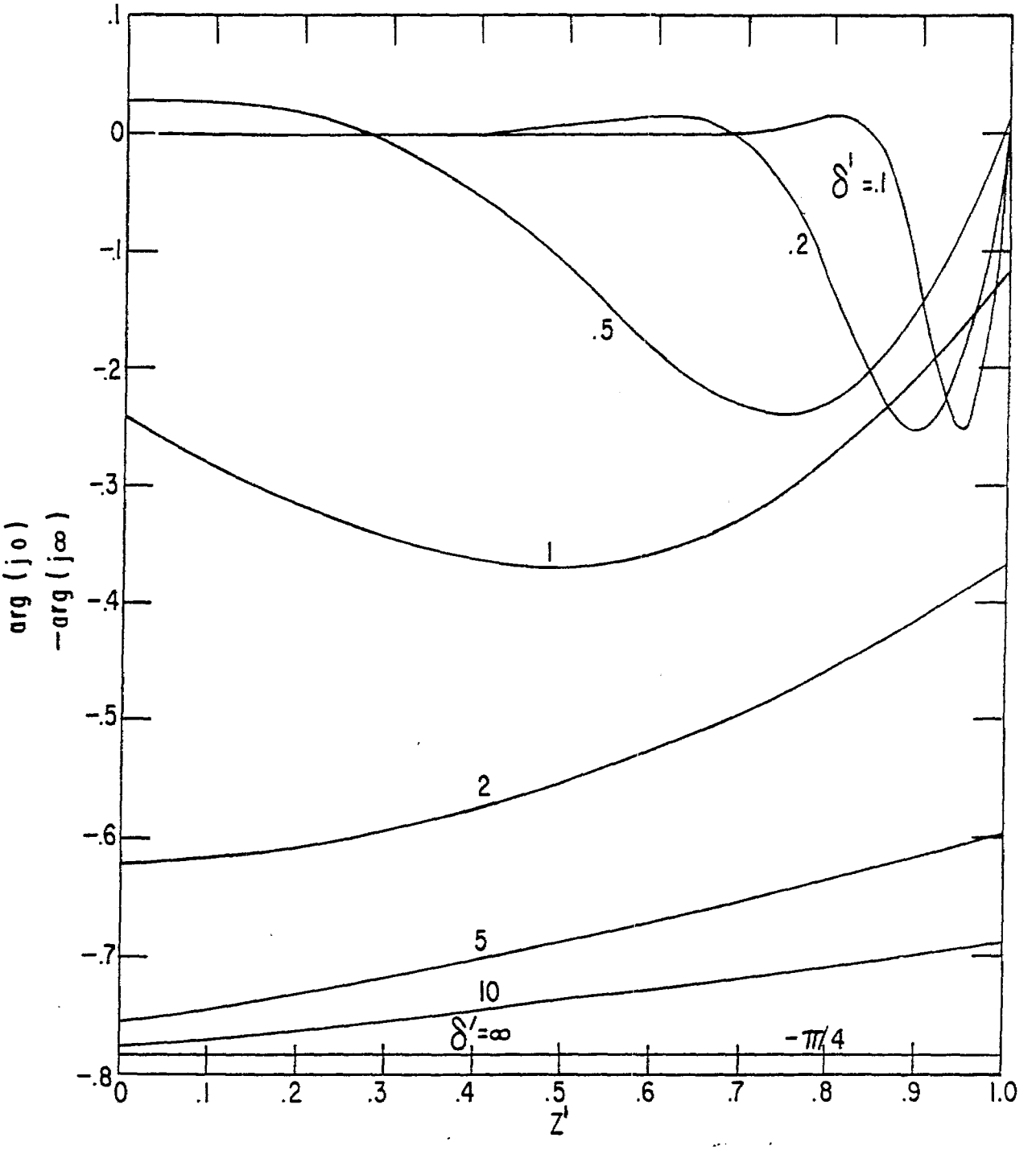

FIGURE II. PHASE CHANGE OF CURRENT DENSITY VS. DEPTH FOR OPEN-CIRCUITED TRANSMISSION LINE

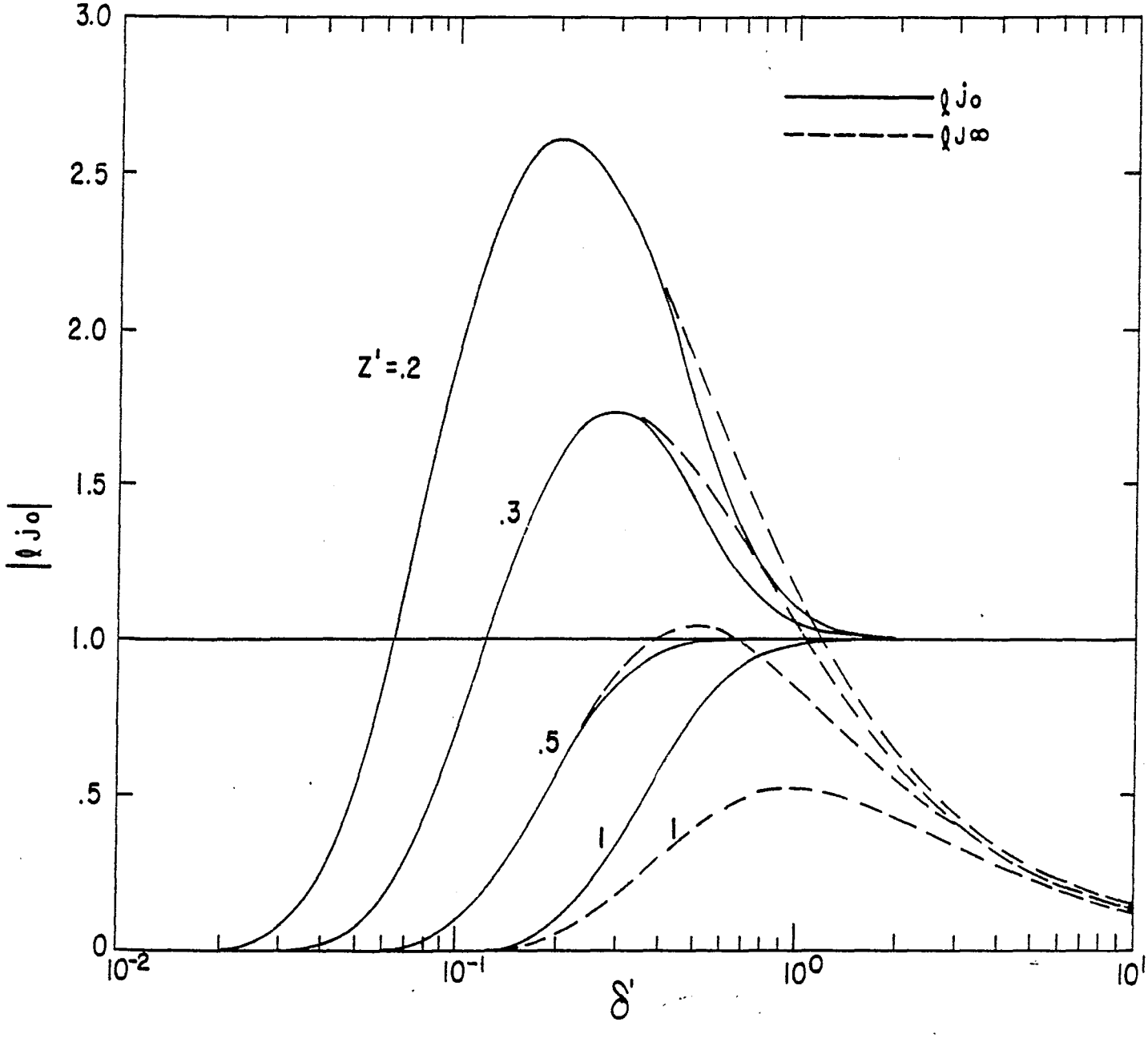

FIGURE 12. NORMALIZED MAGNITUDE OF CURRENT DENSITY VS. SKIN DEPTH FOR OPEN-CIRCUITED TRANSMISSION LINE

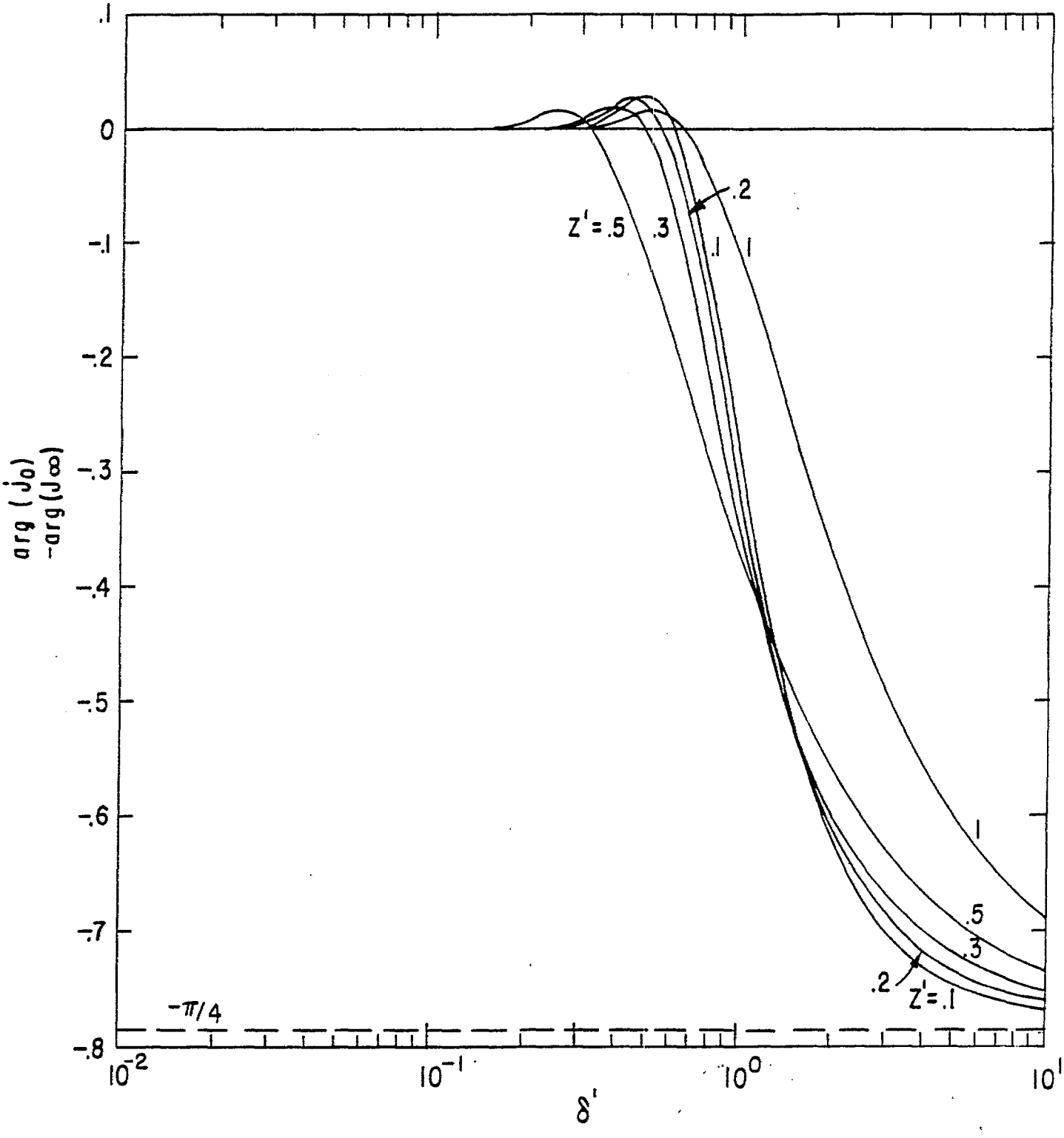

FIGURE 13 PHASE CHANGE OF CURRENT DENSITY VS. SKIN DEPTH FOR OPEN-CIRCUITED TRANSMISSION LINE

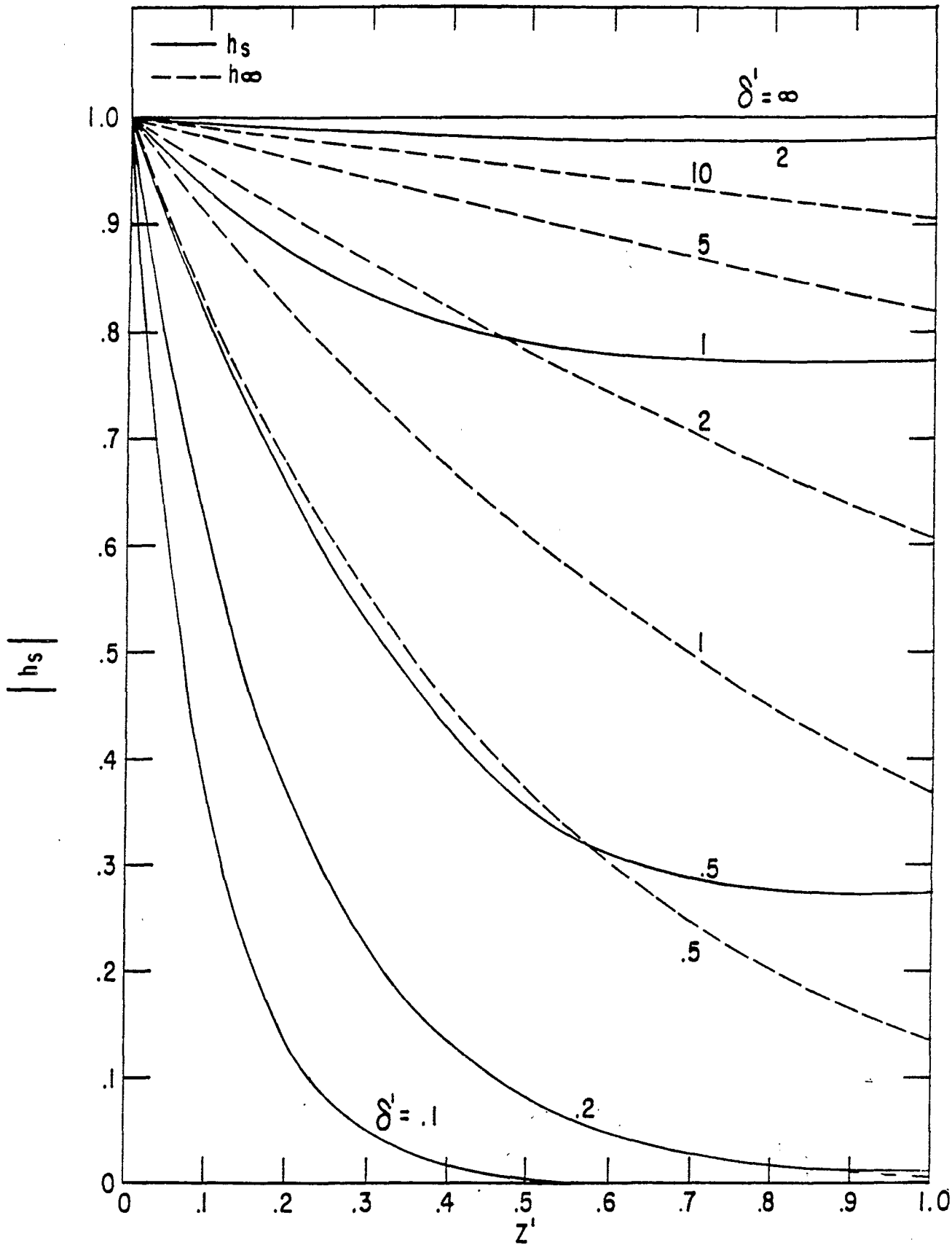

FIGURE 14 NORMALIZED MAGNITUDE OF MAGNETIC FIELD VS DEPTH FOR SHORT-CIRCUITED TRANSMISSION LINE

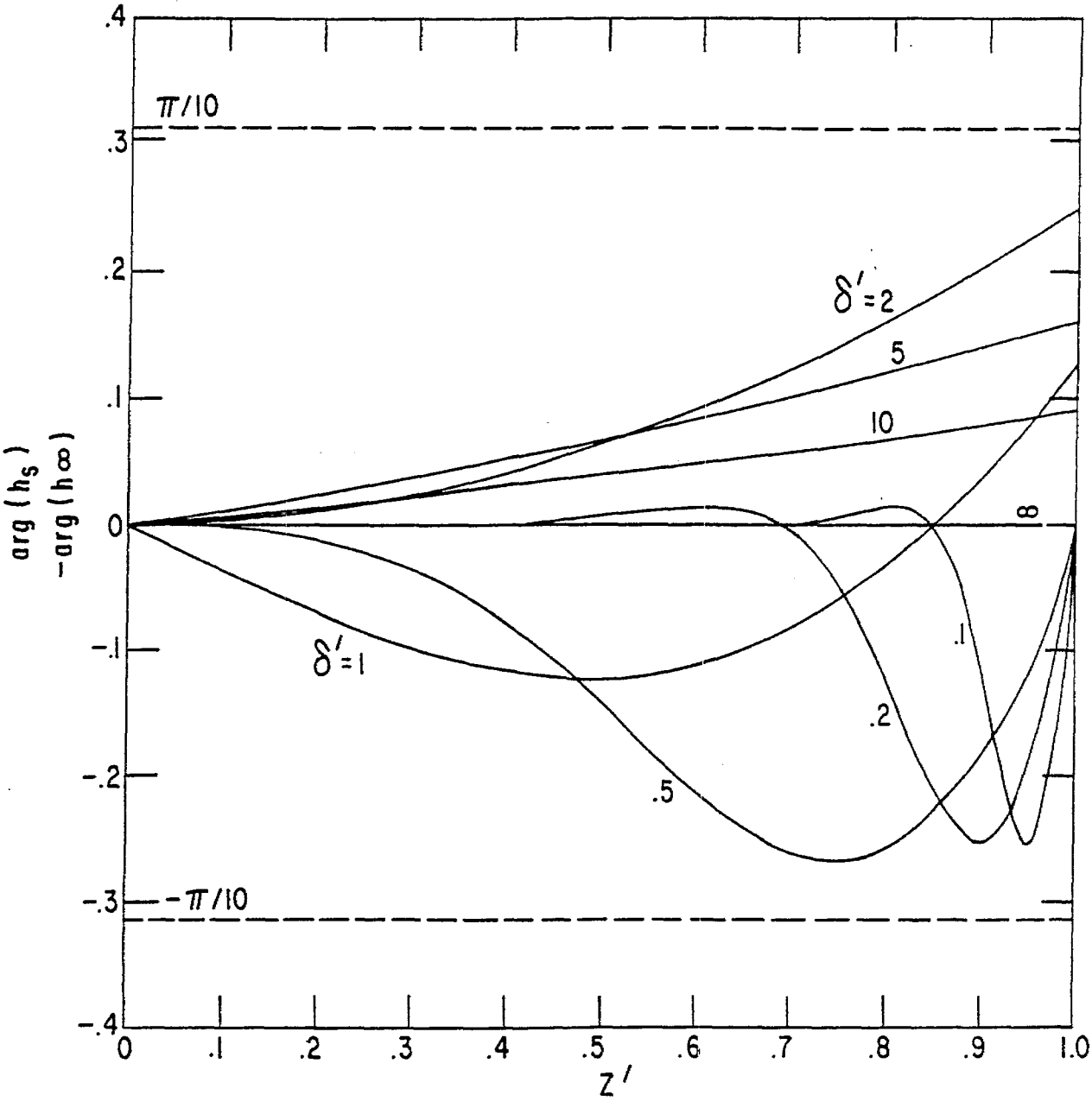

FIGURE 15. PHASE CHANGE OF MAGNETIC FIELD VS DEPTH FOR SHORT-CIRCUITED TRANSMISSION LINE

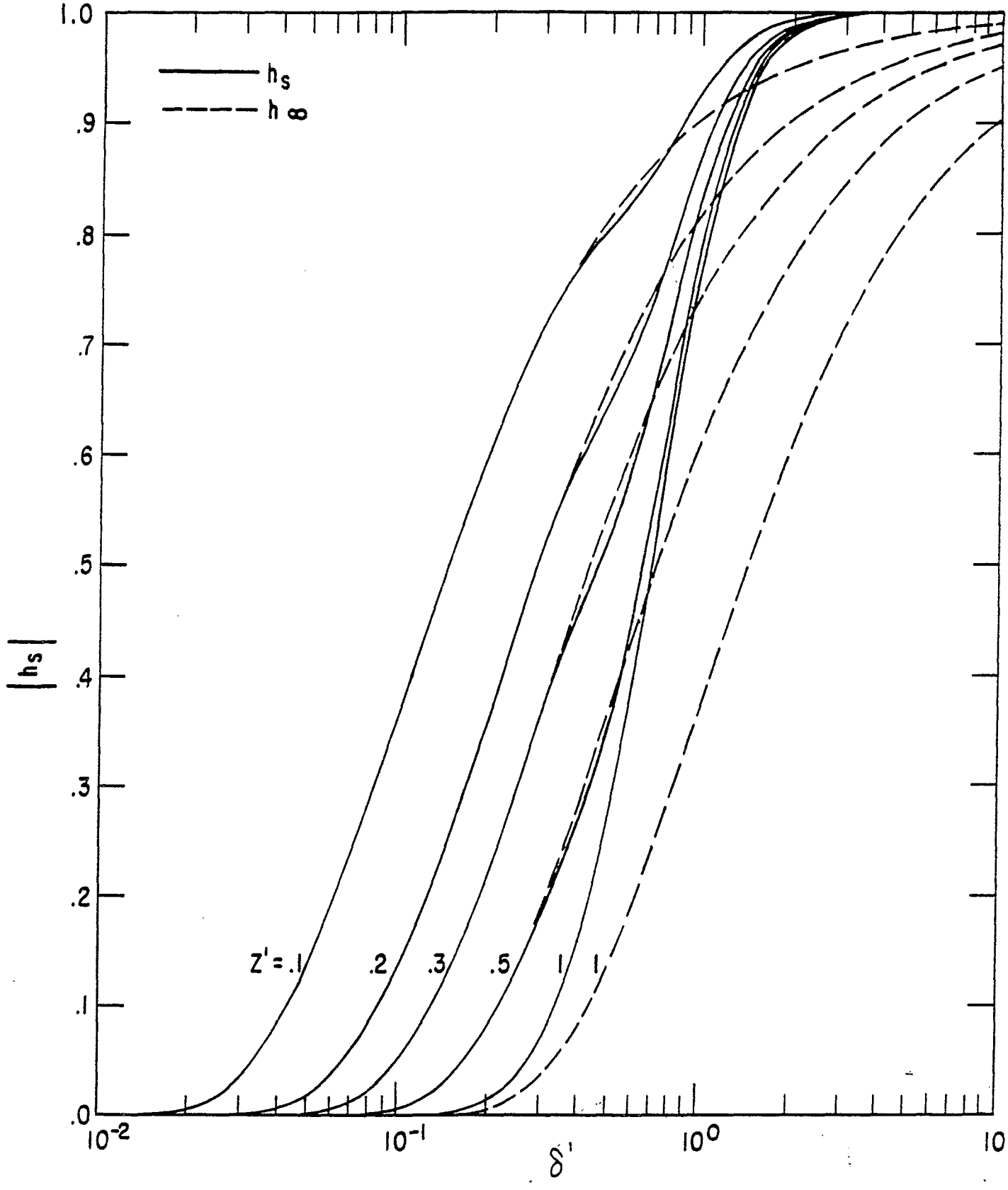

FIGURE 16 NORMALIZED MAGNITUDE OF MAGNETIC FIELD VS. SKIN DEPTH FOR SHORT-CIRCUITED TRANSMISSION LINE

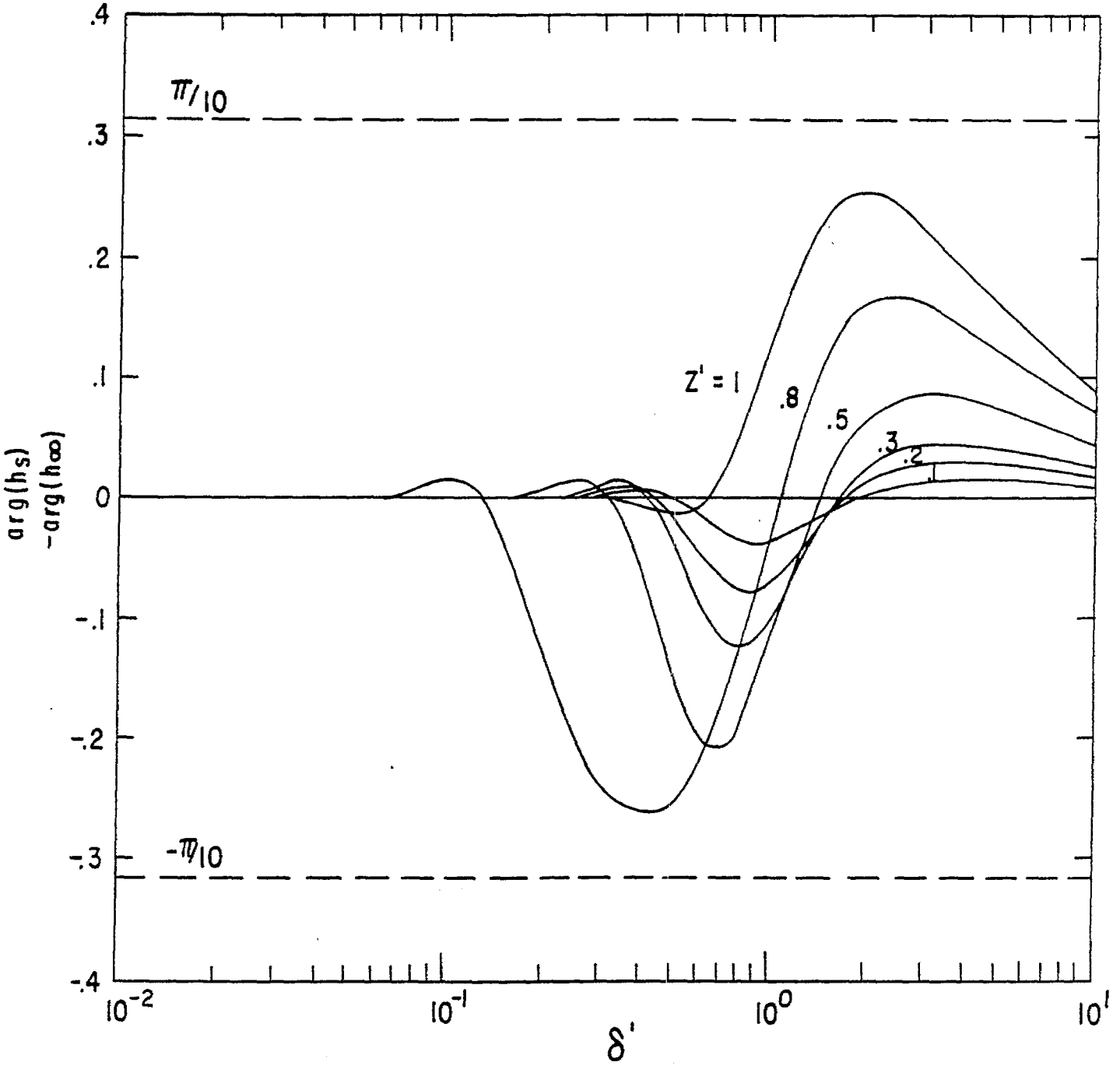

FIGURE 17 PHASE CHANGE OF MAGNETIC FIELD VS SKIN DEPTH FOR SHORT-CIRCUITED TRANSMISSION LINE

unity) the two normalized fields diverge somewhat except near z'=0. Thus, considering the magnetic field distribution the short-circuited transmission line seems somewhat better than the open-circuited transmission line, although practically the former may be somewhat more difficult to construct.

The current density (or electric field) on the short-circuited transmission line has a negative one reflection at the bottom giving (from equations (15) and (32))

$$\ell j_s(z') \approx \frac{e^{jkz} - e^{-jk(2\ell+z)}}{1 - e^{-jk2\ell}} \left(\frac{\ell\sigma}{f_g} Z_{L_s}\right) \tag{39}$$

or

$$\ell j_s(z') \approx \frac{1+j}{\delta'} e^{-(1+j)\frac{z'}{\delta'}} \frac{1 - e^{-2\frac{1+j}{\delta'}(1-z')}}{1 + e^{-2\frac{1+j}{\delta'}}} \tag{40}$$

This is compared with j_∞ in figures 18 through 21. Again j_s and j_∞ are about the same for small δ', except near z'=1 where j_s is zero. However, for large δ', j_s falls much faster than j_∞. For large δ' the short-circuited transmission line (as well as the open-circuited transmission line) does not have the same ratio of current density to magnetic field as does the infinite-length transmission line.

Thus, for small δ' both finite-length transmission lines approximate the "ideal" field distribution characteristics, except near z'=1. However, for large δ' the electric and magnetic fields are not in the desired ratio (in either case). Also for large δ' the field distribution with depth varies, in some cases, from the "ideal" distribution. However, if we make ℓ sufficiently deeper than depths of interest for EMP simulation, the last problem can be alleviated.

IV. Fields in the Time Domain

Next consider the field distributions on the transmission line in the time domain. For convenience we assume a unit step magnetic field at the top of the transmission line, or using the Laplace transform notation we have

$$h(0) = \frac{1}{s} \tag{41}$$

As before, we use subscripts to denote which type of transmission line is being considered. Besides assuming that $\sigma >> \omega\varepsilon$ for frequencies (or times) of interest and that the electrical parameters, μ and σ, do not significantly vary over the extent of the transmission line, we also assume that these latter parameters are independent of frequency (for frequencies of interest).

Keeping the normalized parameters in mind define a characteristic time, t_ℓ, for diffusion of fields on the finite-length transmission line as

$$t_\ell = \frac{\mu\sigma\ell^2}{4} \tag{42}$$

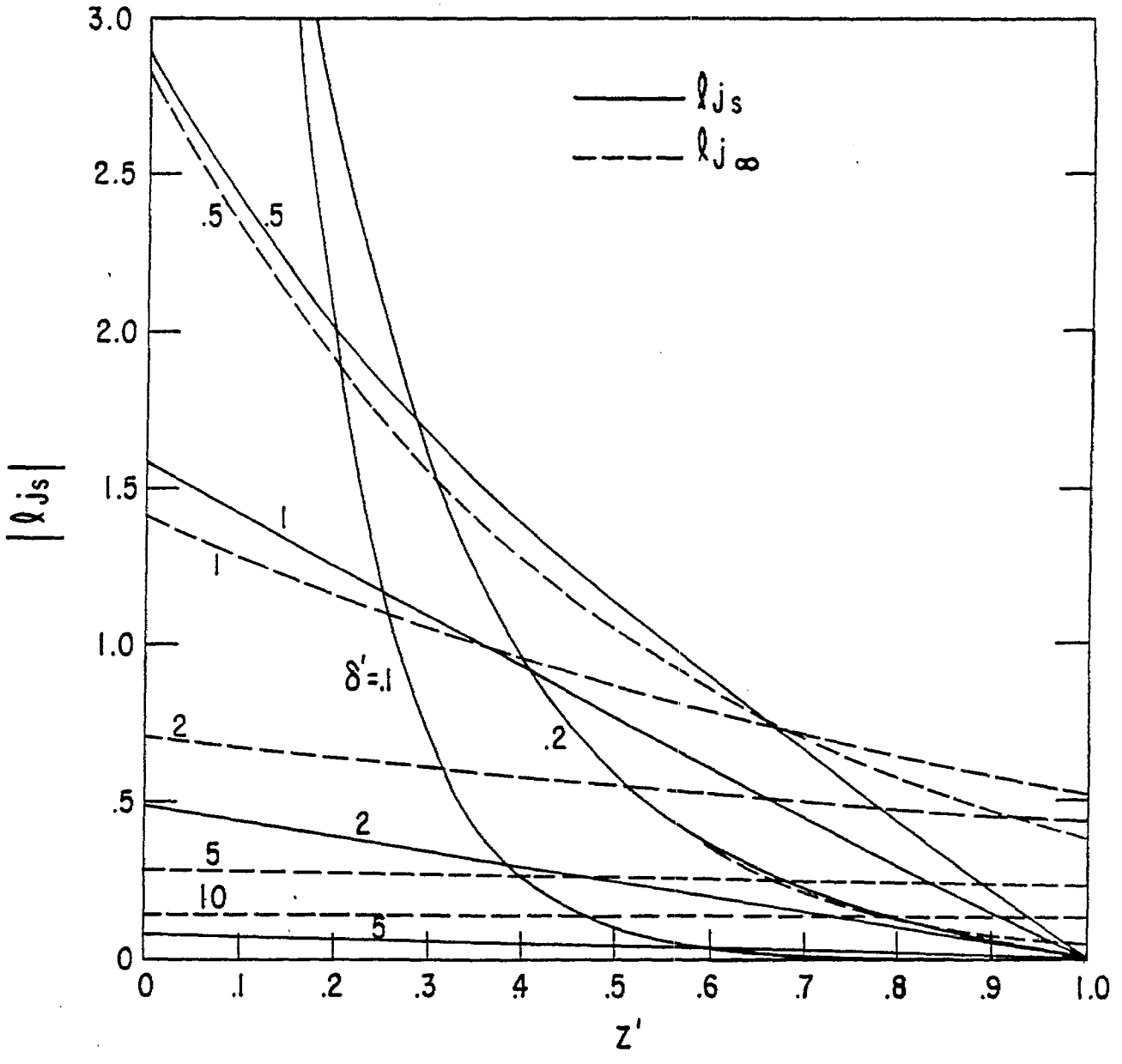

FIGURE 18. NORMALIZED MAGNITUDE OF CURRENT DENSITY VS DEPTH FOR SHORT-CIRCUITED TRANSMISSION LINE

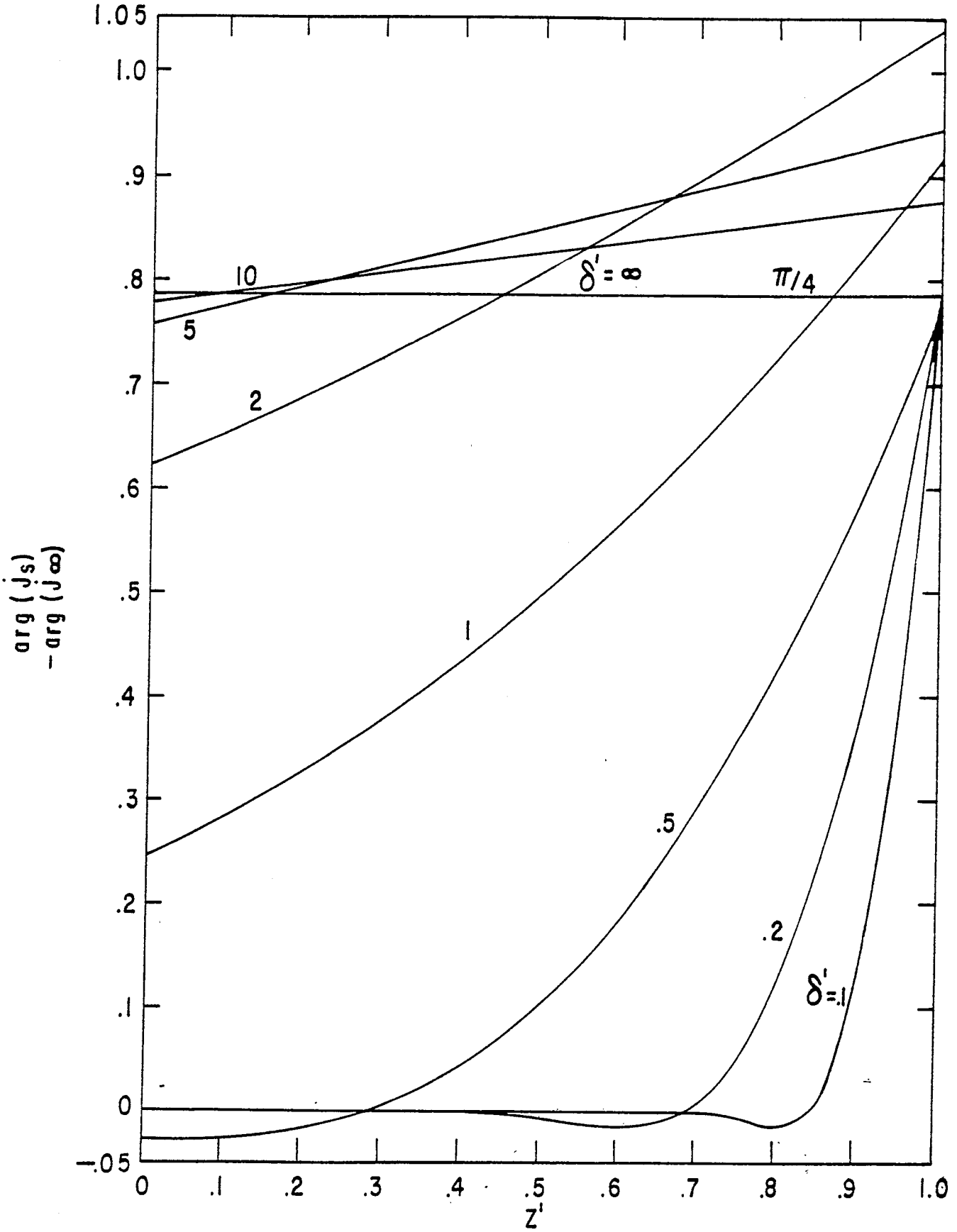

FIGURE 19 PHASE CHANGE OF CURRENT DENSITY VS. DEPTH FOR SHORT-CIRCUITED TRANSMISSION LINE

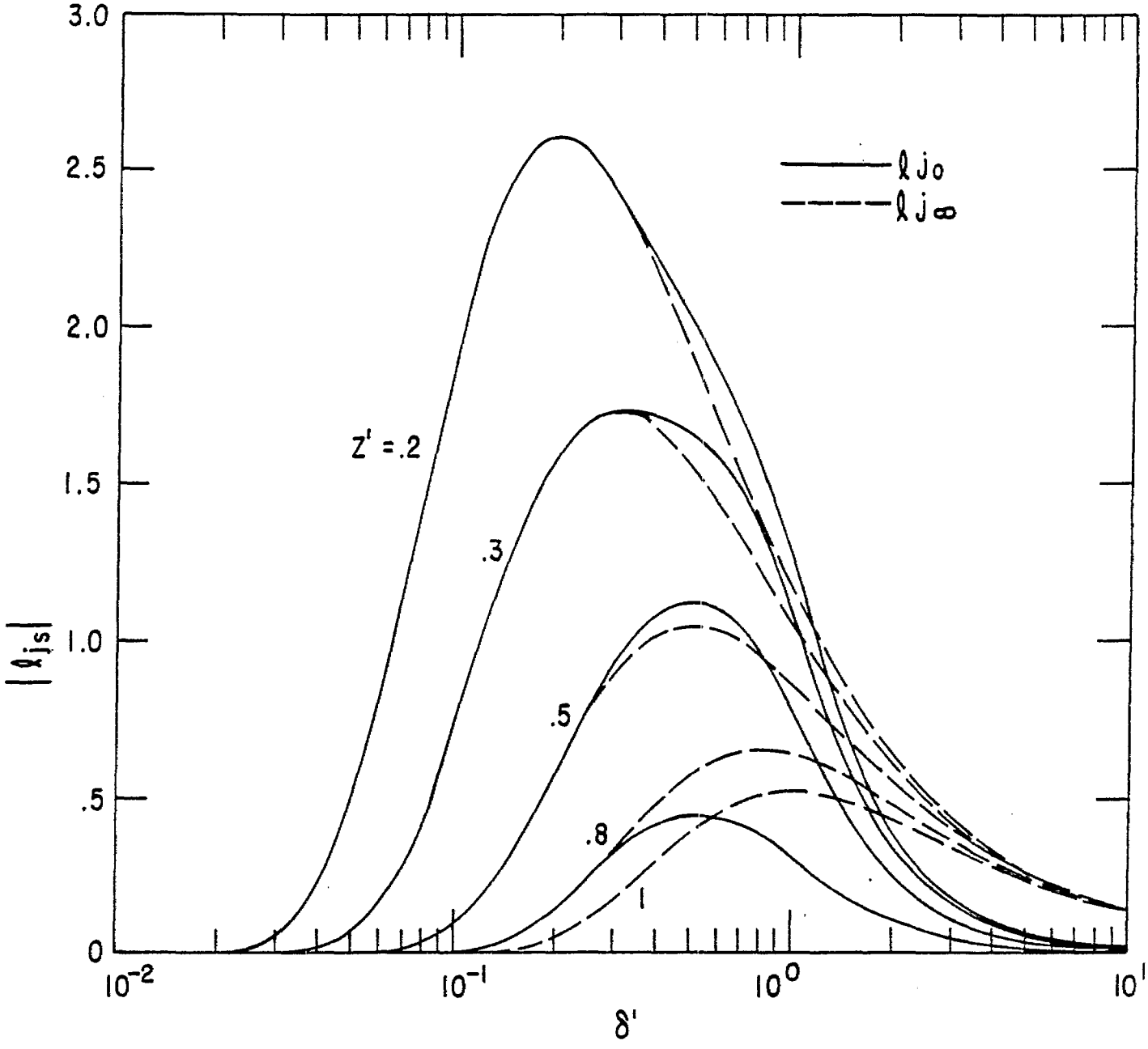

FIGURE 20 NORMALIZED MAGNITUDE OF CURRENT DENSITY VS. SKIN DEPTH FOR SHORT-CIRCUITED TRANSMISSION LINE.

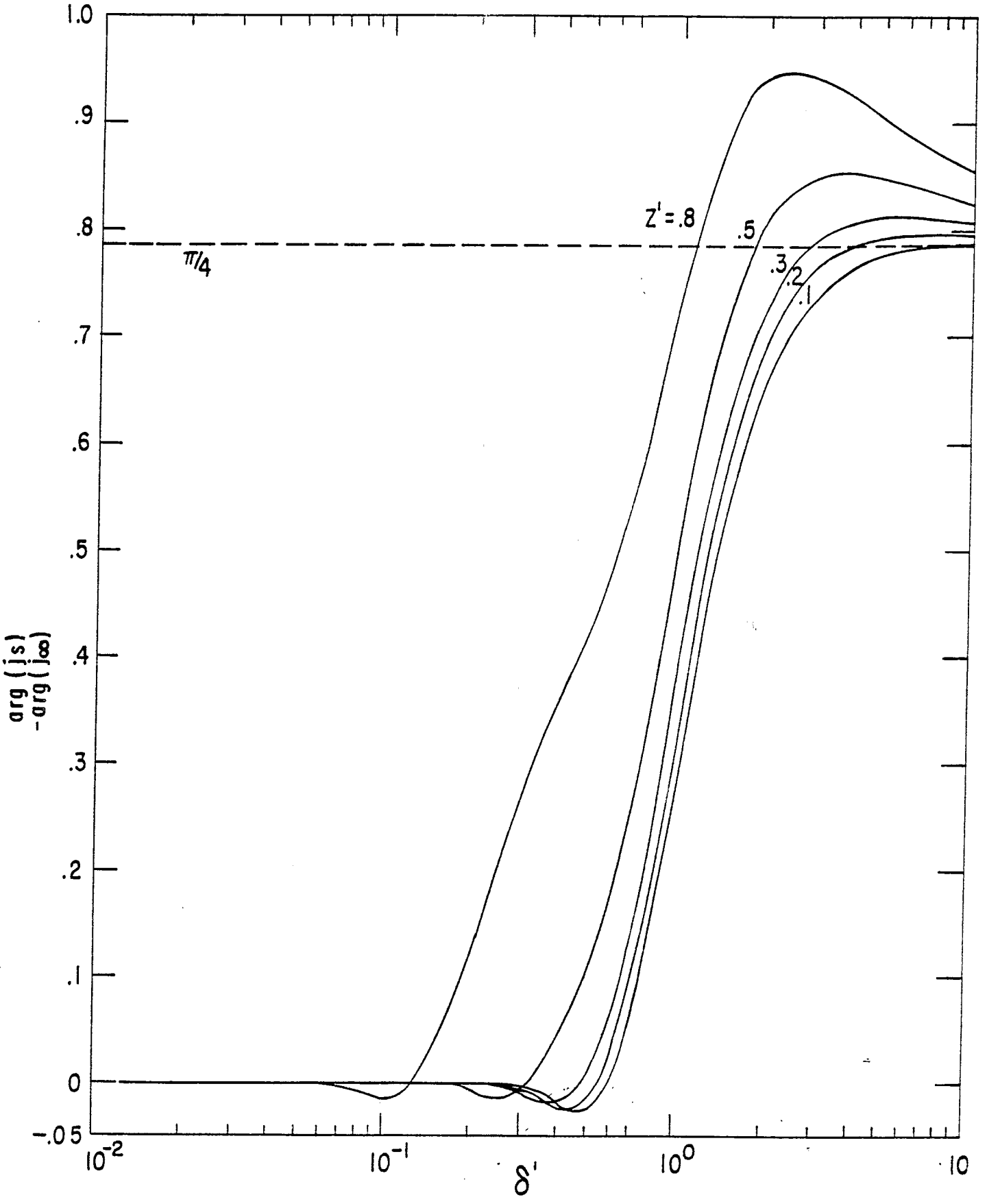

FIGURE 21 PHASE CHANGE OF CURRENT DENSITY VS. SKIN DEPTH FOR SHORT-CIRCUITED TRANSMISSION LINE

and also define a normalized time, τ_ℓ, as

$$\tau_\ell = \frac{t}{t_\ell} \tag{43}$$

Then on the infinite-length transmission line we have for the magnetic field

$$h_\infty(z') = \frac{1}{s} e^{jkz} \tag{44}$$

or from equation (5)

$$h_\infty(z') = \frac{1}{s} e^{\sqrt{s\mu\sigma}\, z} = \frac{1}{s} e^{-2\sqrt{st_\ell}\, z'} \tag{45}$$

In the time domain we then have[3]

$$h_\infty(z') = \text{erfc}\left(z'\sqrt{\frac{t_\ell}{t}}\right) = \text{erfc}\left(\frac{z'}{\sqrt{\tau_\ell}}\right) \tag{46}$$

For the current density we have from equation (4)

$$\ell j_\infty(z') = \ell \sigma Z h_\infty(z') = \ell \sqrt{s\mu\sigma}\; h_\infty(z') \tag{47}$$

and from equation (45)

$$\ell j_\infty(z') = \ell \left(\frac{\mu\sigma}{s}\right)^{1/2} e^{-2\sqrt{st_\ell}\, z'} = 2\left(\frac{t_\ell}{s}\right)^{1/2} e^{-2\sqrt{st_\ell}\, z'} \tag{48}$$

In the time domain we have

$$\ell j_\infty(z') = 2\left(\frac{t_\ell}{\pi t}\right)^{1/2} e^{-\frac{z'^2 t_\ell}{t}} = \frac{2}{\sqrt{\pi\tau_\ell}} e^{-\frac{z'^2}{\tau_\ell}} \tag{49}$$

For the open-circuited transmission line we can modify the results of equation (35) to obtain the magnetic field distribution as

$$h_o(z') = \frac{1}{s} \frac{e^{jkz} - e^{-jk(2\ell+z)}}{1 - e^{-jk2\ell}} \tag{50}$$

or

$$h_o(z') = \frac{1}{s} \frac{e^{-2\sqrt{st_\ell}\, z'} - e^{-2\sqrt{st_\ell}\,(2-z')}}{1 - e^{-4\sqrt{st_\ell}}} \tag{51}$$

Expanding the denominator in an infinite series we have

3. For the Laplace Transforms and function definitions see AMS 55, Handbook of Mathematical Functions, National Bureau of Standards, 1964. For convenience the same symbol is used for both a function and its Laplace transform but which use is intended in a particular case should be apparent.

$$h_o(z') \approx \frac{1}{s}\left[e^{-2\sqrt{st_\ell}z'} - e^{-2\sqrt{st_\ell}(2-z')}\right]\sum_{n=0}^{\infty} e^{-4n\sqrt{st_\ell}} \tag{52}$$

or

$$h_o(z') \approx \frac{1}{s}\sum_{n=0}^{\infty}\left[e^{-2(z'+2n)\sqrt{st_\ell}} - e^{-2(-z'+2(n+1))\sqrt{st_\ell}}\right] \tag{53}$$

Inverting the transform term by term we have in the time domain

$$h_o(z') \approx \sum_{n=0}^{\infty}\left[\operatorname{erfc}\left(\frac{(z'+2n)\sqrt{t_\ell}}{\sqrt{t}}\right) - \operatorname{erfc}\left(\frac{(-z'+2(n+1)\sqrt{t_\ell}}{\sqrt{t}}\right)\right] \tag{54}$$

or

$$h_o(z') \approx \sum_{n=0}^{\infty}\left[\operatorname{erfc}\left(\frac{z'+2n}{\sqrt{\tau_\ell}}\right) - \operatorname{erfc}\left(\frac{-z'+2(n+1)}{\sqrt{\tau_\ell}}\right)\right] \tag{55}$$

This is plotted in figure 22 and compared with h_∞. For τ_ℓ small compared to one the two distributions are about the same (except near $z'=1$) but for τ_ℓ large compared to one h_o decreases with increasing z', becoming zero at $z'=1$. This is the same characteristic noted for large δ' in the previous section.

The current density on the open-circuited transmission for the assumed unit step magnetic field can be obtained by modifying the results of equation (36) as

$$\ell j_o(z') \approx \frac{1}{s}\left(\frac{\ell\sigma}{f_g} Z_{L_o}\right)\frac{e^{jkz} + e^{-jk(2\ell+z)}}{1 + e^{-jk2\ell}} \approx \ell\left(\frac{u\sigma}{s}\right)^{1/2}\frac{e^{-2\sqrt{st_\ell}z'} + e^{-2\sqrt{st_\ell}(2-z')}}{1 - e^{-4\sqrt{st_\ell}}} \tag{56}$$

or

$$\ell j_o(z') \approx 2\left(\frac{t_\ell}{s}\right)^{1/2}\frac{e^{-2\sqrt{st_\ell}z'} + e^{-2\sqrt{st_\ell}(2-z')}}{1 - e^{-4\sqrt{st_\ell}}} \tag{57}$$

Expanding the denominator

$$\ell j_o(z') \approx 2\left(\frac{t_\ell}{s}\right)^{1/2}\left[e^{-2\sqrt{st_\ell}z'} + e^{-2\sqrt{st_\ell}(2-z')}\right]\sum_{n=0}^{\infty} e^{-4n\sqrt{st_\ell}} \tag{58}$$

or

$$\ell j_o(z') \approx 2\left(\frac{t_\ell}{s}\right)^{1/2}\sum_{n=0}^{\infty}\left[e^{-2(z'+2n)\sqrt{st_\ell}} + e^{-2(-z'+2(n+1))\sqrt{st_\ell}}\right] \tag{59}$$

Converting to the time domain

$$\ell j_o(z') \approx 2\left(\frac{t_\ell}{\pi t}\right)^{1/2}\sum_{n=0}^{\infty}\left[e^{-\frac{(z'+2n)^2 t_\ell}{t}} + e^{-\frac{(-z'+2(n+1))^2 t_\ell}{t}}\right] \tag{60}$$

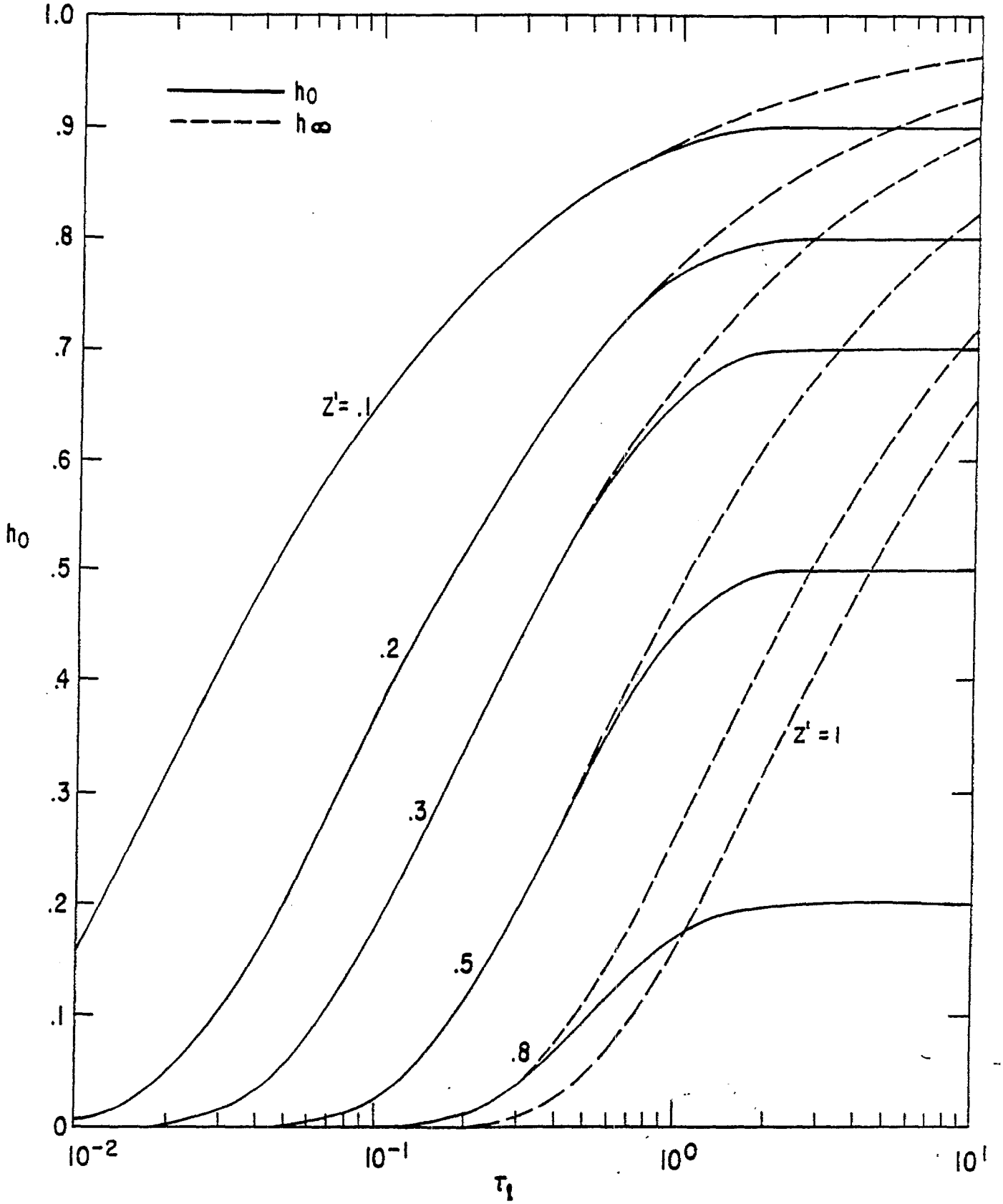

FIGURE 22 UNIT STEP RESPONSE OF MAGNETIC FIELD VS. NORMALIZED TIME FOR OPEN-CIRCUITED TRANSMISSION LINE

or

$$\ell j_o(z') \approx \frac{2}{\sqrt{\pi\tau_\ell}} \sum_{n=0}^{\infty} \left[e^{-\frac{(z'+2n)^2}{\tau_\ell}} + e^{-\frac{(-z'+2(n+1))^2}{\tau_\ell}} \right] \tag{61}$$

This is plotted in figure 23 and compared with j_∞. Again for small τ_ℓ the two distributions are about the same (except near $z'=1$). However, (as noted for large δ') for large τ_ℓ, j_o tends to one while j_∞ tends to zero.

On the short-circuited transmission line the magnetic field distribution is (modifying equation (38))

$$h_s(z') = \frac{1}{s} \frac{e^{jkz} + e^{-jk(2\ell+z)}}{1 + e^{-jk2\ell}} \tag{62}$$

or

$$h_s(z') \approx \frac{1}{s} \frac{e^{-2\sqrt{st_\ell}\,z'} + e^{-2\sqrt{st_\ell}(2-z')}}{1 + e^{-4\sqrt{st_\ell}}} \tag{63}$$

Expanding the denominator

$$h_s(z') \approx \frac{1}{s} \left[e^{-2\sqrt{st_\ell}\,z'} + e^{-2\sqrt{st_\ell}(2-z')} \right] \sum_{n=0}^{\infty} (-1)^n e^{-4n\sqrt{st_\ell}} \tag{64}$$

or

$$h_s(z') \approx \frac{1}{s} \sum_{n=0}^{\infty} (-1)^n \left[e^{-2(z'+2n)\sqrt{st_\ell}} + e^{-2(-z'+2(n+1))\sqrt{st_\ell}} \right] \tag{65}$$

Converting to the time domain

$$h_s(z') \approx \sum_{n=0}^{\infty} (-1)^n \left[\operatorname{erfc}\left(\frac{(z'+2n)\sqrt{t_\ell}}{\sqrt{t}} \right) + \operatorname{erfc}\left(\frac{(-z'+2(n+1))\sqrt{t_\ell}}{\sqrt{t}} \right) \right] \tag{66}$$

or

$$h_s(z') \approx \sum_{n=0}^{\infty} (-1)^n \left[\operatorname{erfc}\left(\frac{z'+2n}{\sqrt{\tau_\ell}} \right) + \operatorname{erfc}\left(\frac{-z'+2(n+1)}{\sqrt{\tau_\ell}} \right) \right] \tag{67}$$

This is plotted in figure 24 and compared with h_∞. For small τ_ℓ the two distributions are about the same (except near $z'=1$), but for large τ_ℓ (as for large δ'), h_s approaches one faster than h_∞.

The corresponding current density on the short-circuited transmission line is (modifying equation (39))

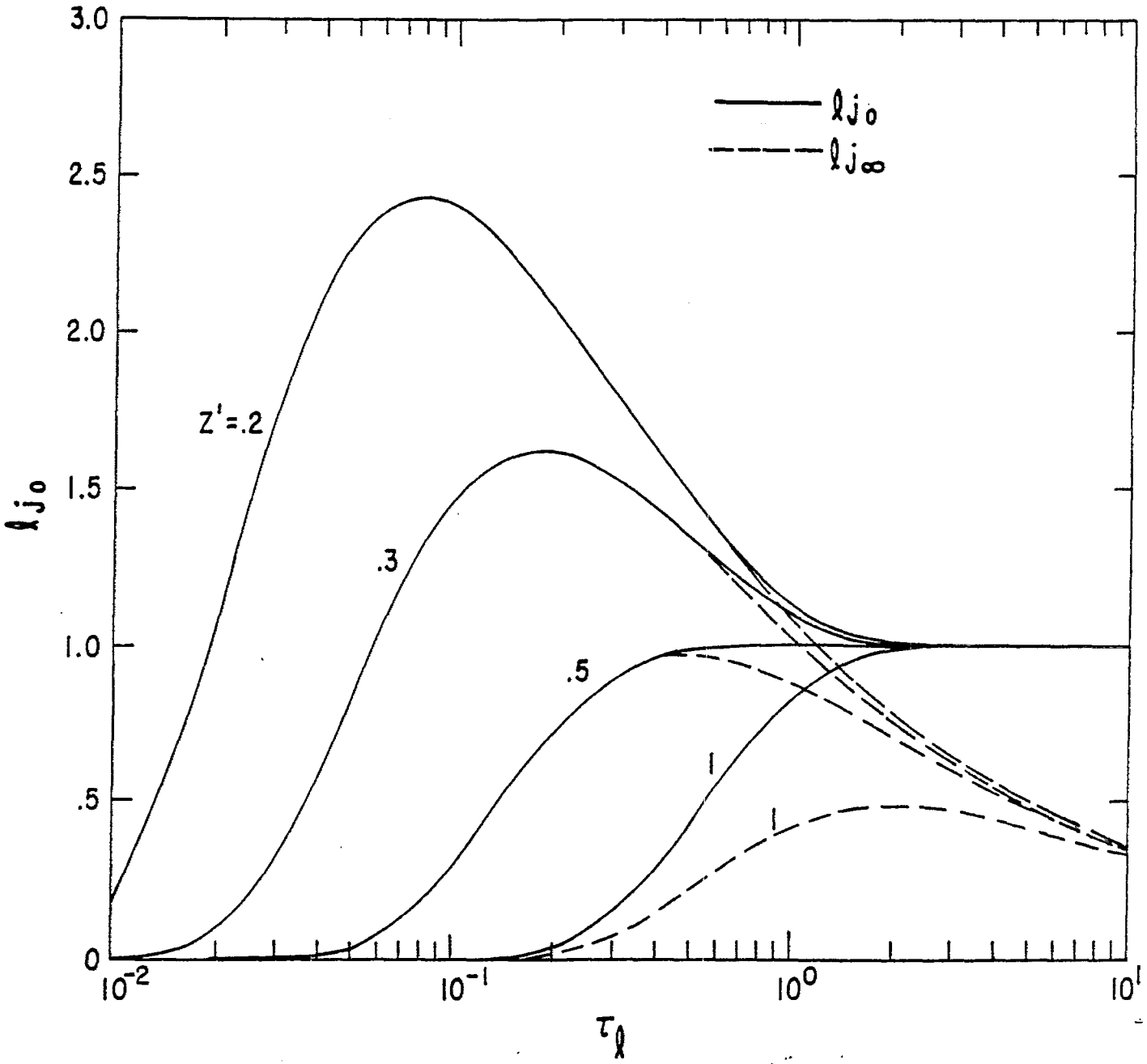

FIGURE 23 RESPONSE OF NORMALIZED CURRENT DENSITY TO STEP MAGNETIC FIELD VS NORMALIZED TIME FOR OPEN-CIRCUITED TRANSMISSION LINE

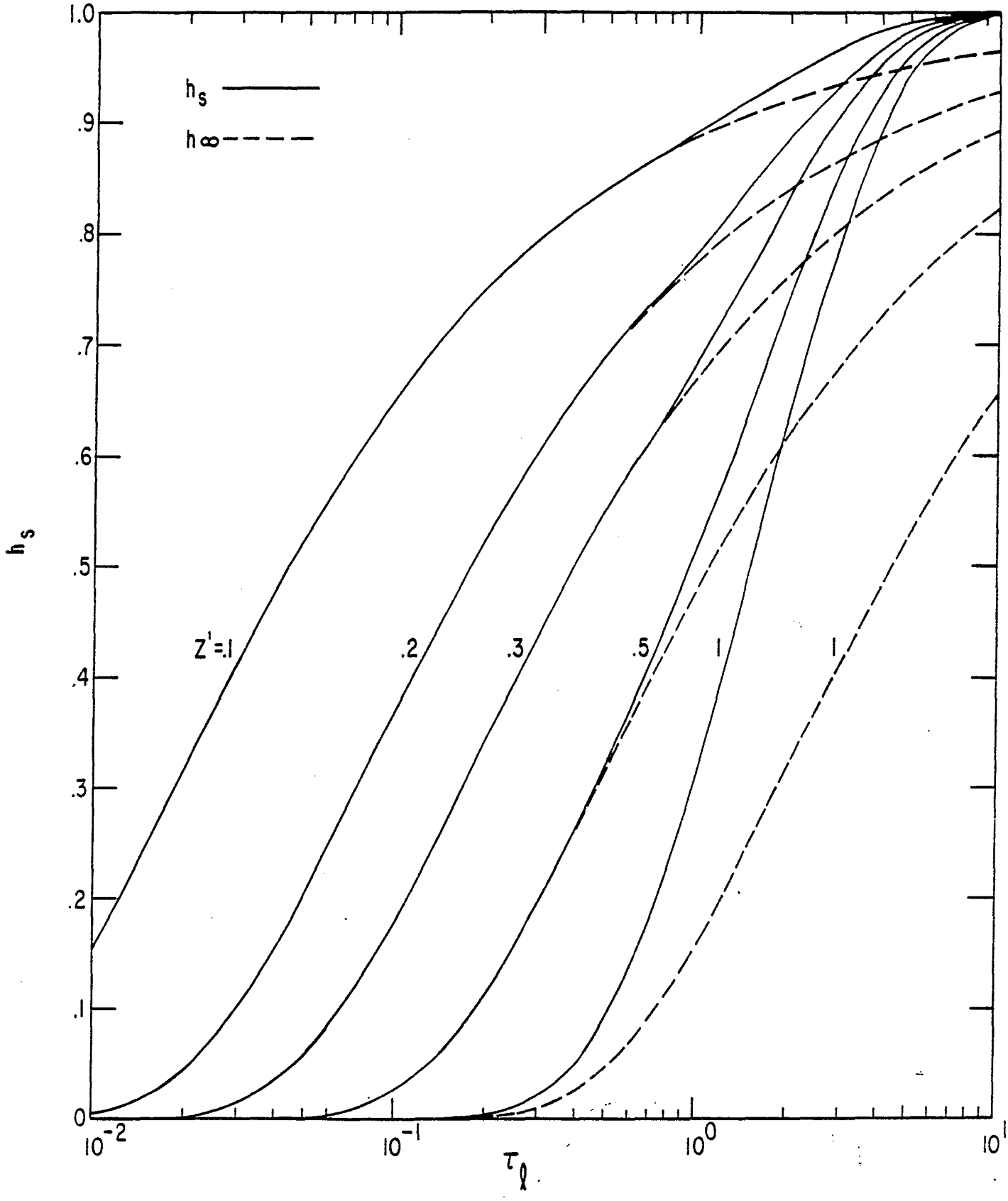

FIGURE 24. UNIT STEP RESPONSE OF MAGNETIC FIELD VS. NORMALIZED TIME FOR SHORT-CIRCUITED TRANSMISSION LINE

$$\ell j_s(z') = \frac{1}{s}\left(\frac{\ell\sigma}{f_g} Z_{L_s}\right) \frac{e^{jkz} - e^{-jk(2\ell+z)}}{1 - e^{-jk2\ell}} = \ell\left(\frac{\mu\sigma}{s}\right)^{1/2} \frac{e^{-2\sqrt{st_\ell}z'} - e^{-2\sqrt{st_\ell}(2-z')}}{1 + e^{-4\sqrt{st_\ell}}} \tag{68}$$

or

$$\ell j_s(z') = 2\left(\frac{t_\ell}{s}\right)^{1/2} \frac{e^{-2\sqrt{st_\ell}z'} - e^{-2\sqrt{st_\ell}(2-z')}}{1 + e^{-4\sqrt{st_\ell}}} \tag{69}$$

Expanding the denominator

$$\ell j_s(z') = 2\left(\frac{t_\ell}{s}\right)^{1/2} \left[e^{-2\sqrt{st_\ell}z'} - e^{-2\sqrt{st_\ell}(2-z')}\right] \sum_{n=0}^{\infty} (-1)^n e^{-4n\sqrt{st_\ell}} \tag{70}$$

or

$$\ell j_s(z') = 2\left(\frac{t_\ell}{s}\right)^{1/2} \sum_{n=0}^{\infty} (-1)^n \left[e^{-2(z'+2n)\sqrt{st_\ell}} - e^{-2(-z'+2(n+1))\sqrt{st_\ell}}\right] \tag{71}$$

Converting to the time domain

$$\ell j_s(z') = 2\left(\frac{t_\ell}{\pi t}\right)^{1/2} \sum_{n=0}^{\infty} (-1)^n \left[e^{-\frac{(z'+2n)^2 t_\ell}{t}} - e^{-\frac{(-z'+2(n+1))^2 t_\ell}{t}}\right] \tag{72}$$

or

$$\ell j_s(z') = \frac{2}{\sqrt{\pi\tau_\ell}} \sum_{n=0}^{\infty} (-1)^n \left[e^{-\frac{(z'+2n)^2}{\tau_\ell}} - e^{-\frac{(-z'+2(n+1))^2}{\tau_\ell}}\right] \tag{73}$$

This is plotted in figure 25 and compared with j_∞. For small τ_ℓ the two distributions are about the same (except near $z'=1$), but for large τ_ℓ (as for large δ'), j_s approaches zero much faster than j_∞.

Thus, in the cases considered, the finite-length transmission line reasonably approximates the "ideal" case for times smaller than t_ℓ. However, for times longer than t_ℓ the field distributions change significantly. If we confine our region of interest to near the top of the transmission line the field distributions will approximate the "ideal" case. However, the relationship between the electric and magnetic fields will still be different but in some cases this may not be important.

V. Illustration of Field Distortion by Buried Structure

As discussed in the introduction, one of the limitations on the calculation of the field distributions is the presence of the buried structure undergoing EMP simulation. The field distribution near the buried structure, given a uniform field distribution at distances from the structure large compared to its horizontal dimensions, can be illustrated by an example. Consider the buried structure to be a long conducting circular cylinder of unit radius whose axis is the z axis. This case is illustrated in figure 26 for x and y both positive and is given by the conformal transformation

$$w = z + \frac{1}{z} \tag{74}$$

where

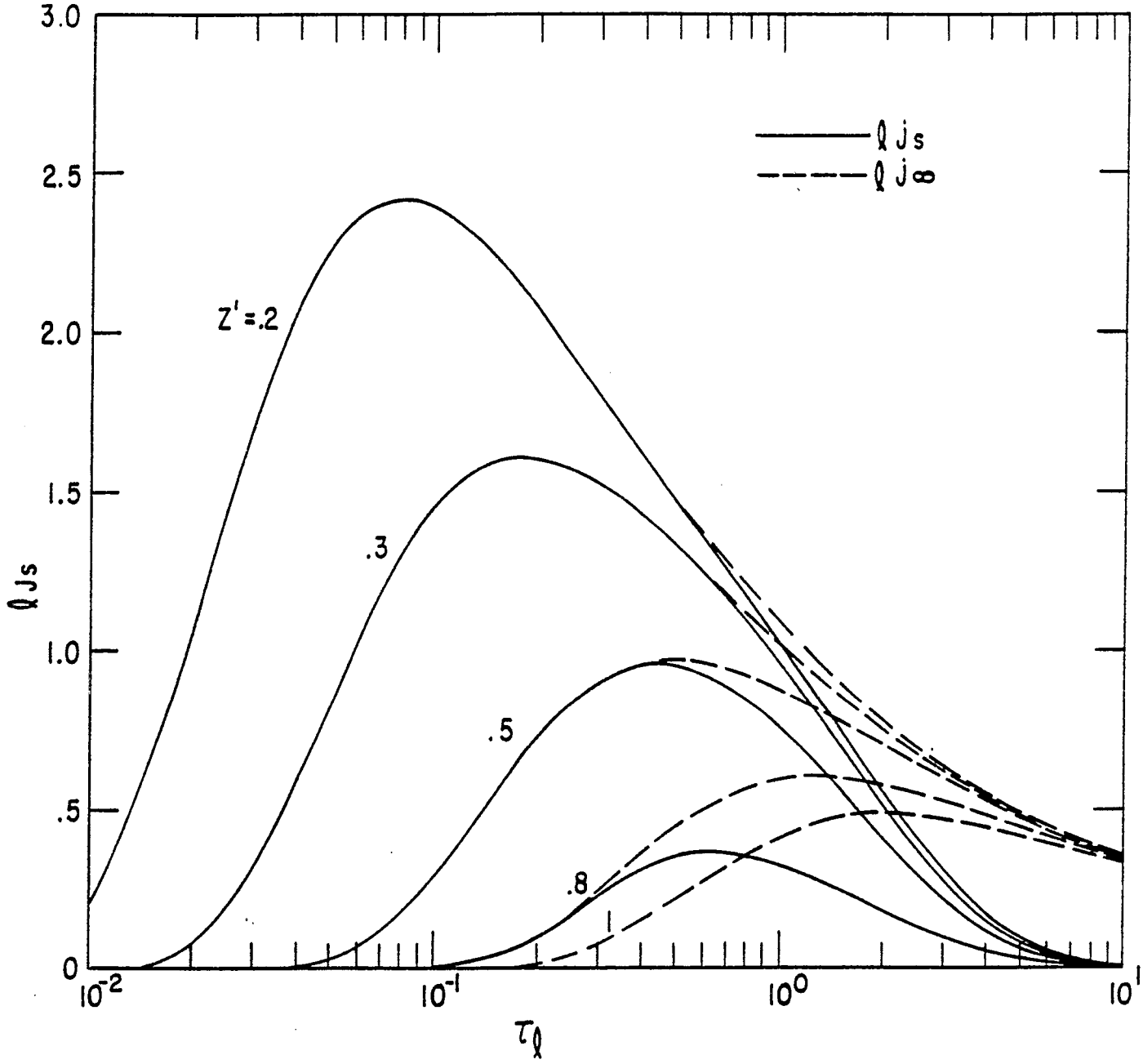

FIGURE 25
RESPONSE OF NORMALIZED CURRENT DENSITY TO STEP MAGNETIC FIELD VS NORMALIZED TIME FOR SHORT-CIRCUITED TRANSMISSION LINE

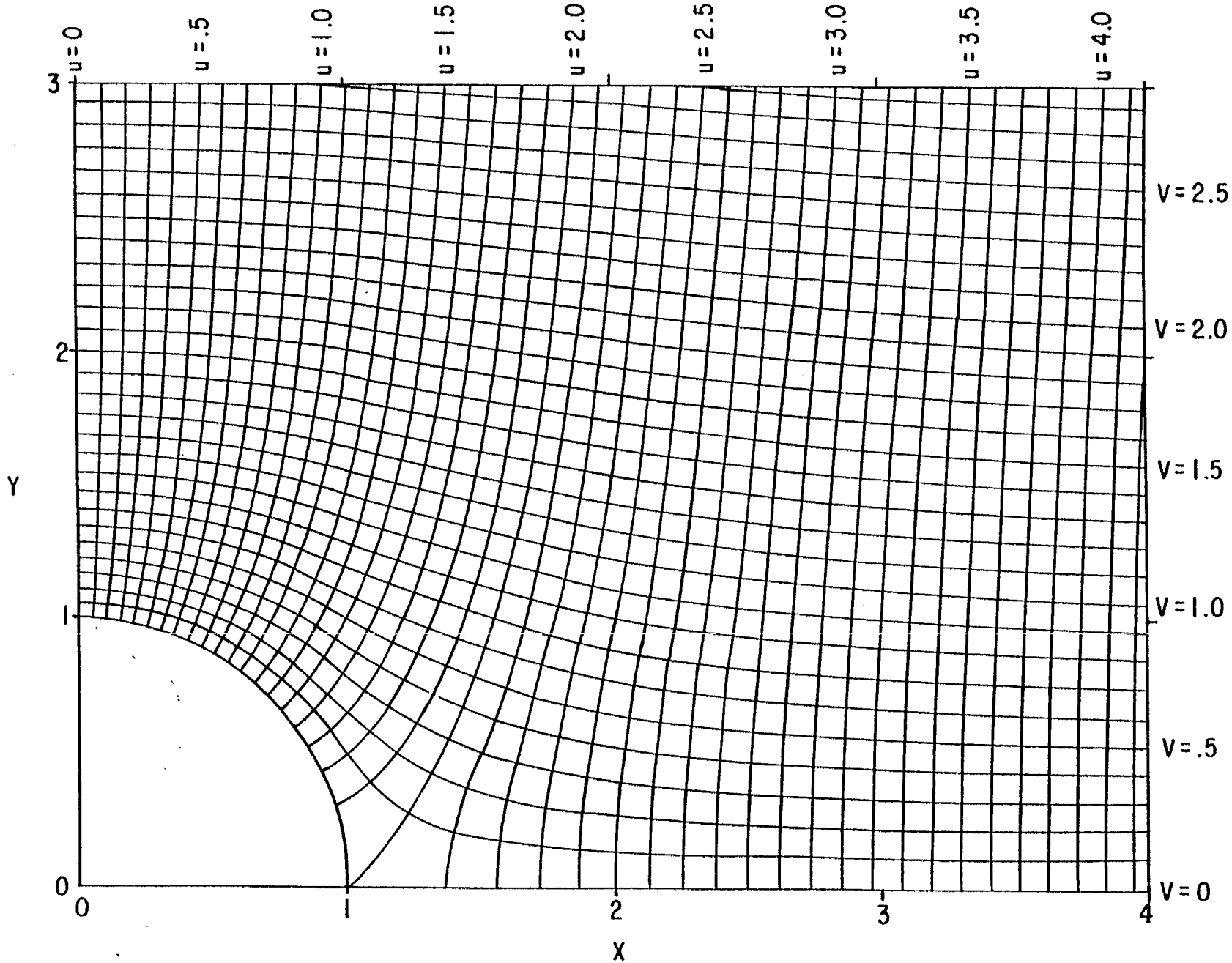

FIGURE 26 FIELD DISTRIBUTION AROUND CONDUCTING CYLINDER

$$z = x + jy \tag{75}$$

and

$$w = u + jv \tag{76}$$

The electric field lines are lines of constant u and the magnetic field lines are lines of constant v where

$$u = x + \frac{x}{x^2+y^2} \tag{77}$$

and

$$v = y - \frac{y}{x^2+y^2} \tag{78}$$

In the approximation that the waves in the ground are propagating in the negative z direction this transformation would represent the field distribution horizontally.

For this special case in which we have a TEM wave propagating into the ground, even in the presence of a field-disturbing structure, we can include it in our transmission-line simulation technique. For example, as in the case illustrated in figure 26, instead of placing two parallel rows of conductors into the ground (as in figure 1), we might place each of these rows along magnetic field lines on each side of the structure. Thus, when we drive these conductors as a transmission line we approximate the altered field distribution in the vicinity of the buried structure. However, if this buried structure does not maintain the same cross section for the full length of the transmission line or at least to the depth to which significant fields (relative to the fields at the surface) extend, then this technique of matching the distorted field structure will be somewhat inaccurate. Likewise, if significant fields penetrate the buried structure (relative to fields external to the structure) and if this penetration is frequency dependent (for frequencies of interest) then the field distribution near the structure is frequency dependent and our transmission line cannot match this for all frequencies.

In those cases where we cannot match the field distribution close to the buried structure with our transmission line, we can try to move it away from the immediate vicinity of the structure into regions where the buried structure does not significantly distort the field. Figure 26 can give us some idea of how far that might be so that we can choose the width, 2a, and spacing, 2b, of our transmission line sufficiently large. However, if the buried structure has a large horizontal extent or has such things as long cables attached to it, the above criterion on transmission-line dimensions may be difficult to meet, requiring a more detailed consideration of the specific case.

VI. Summary

Within certain restrictions, then, the buried transmission line can be used for EMP simulation on buried structures. For frequencies such that the skin depth is less than the length of the transmission lines, the field distribution approximates the anticipated EMP field distribution with frequency and depth. For skin depths larger than the length of the transmission line the field distribution is somewhat distorted, but if we confine our area of interest to near the top of the transmission line this difficulty is overcome. However, in this latter case, the electric and magnetic fields do not have the desired relationship to one another, which may or may not be important in a given case. There are various ways we can try to terminate the finite-length transmission line to try to optimize its characteristics but in many cases the open-circuited transmission line may be the most practical.

There are some other restrictions on the validity of our calculations of the field distributions on the finite-length transmission line. For example, there are fringing fields at both ends of the transmission line. At the top of the transmission line it is desirable (and in many cases necessary) to distribute the connecting conductors from the generator to the buried transmission line in such a manner as to maintain the desired field distribution (as calculated) on the transmission line (especially near the top). It may be difficult to alter the fringing fields at the bottom of the transmission line but this may not be a serious problem in many cases. We have neglected transit times associated with distributing fields over the surface of the ground. We have assumed that the electrical parameters of the soil are independent of position and frequency over the ranges of interest for our calculations but these are only assumptions for convenience which may not necessarily apply to all real cases of interest. Also, the buried structure undergoing EMP simulation will affect the field distribution. If the structure, including the conductors (such as cables) attached to it, is extensive it may be difficult to adequately simulate the EMP field distribution on the structure. However, such cases need individual consideration.

We would like to thank Mr. Robert Mercer who programmed the computer s olutions for the plots contained in this note.